

The University of Melbourne
Department of Mathematics and Statistics.

Physical Combinatorics of Non-Unitary Minimal Models

Hannah Fitzgerald
Honours Thesis

supervisor: Associate Professor Paul Pearce

November 29, 2006

Contents

Introduction	5
1 Forrester-Baxter Lattice Models	7
1.1 Boltzmann Weights and Local Properties	7
1.1.1 Boltzmann weights	7
1.2 One-Dimensional Configurational Sums	8
1.2.1 Local height probabilities and one-dimensional sums	8
1.2.2 Alternate local energies	10
1.3 Double-Row Transfer Matrices	19
2 Conformal Field Theory	21
2.1 Minimal Models	21
2.2 Bosonic Characters	22
2.3 Finitised Characters	24
2.3.1 Continued fraction decomposition	24
2.3.2 Gaussian Polynomials	25
2.3.3 Finitised Fermionic Characters	27
2.3.4 Finitised Bosonic Characters	27
2.3.5 Equivalence of Finitised Characters	28
3 Physical Combinatorics of Critical Forrester-Baxter Models	29
3.1 $\mathcal{M}(2, 5)$	31
3.2 $\mathcal{M}(2, 7)$	35
3.3 $\mathcal{M}(4, 7)$	41
3.4 Duality	46
3.5 Summary of Results	47
Conclusion	48

Introduction

Lattice models are simple mathematical models that describe the behaviour of statistically fluctuating physical systems such as magnets and fluids. The study of these systems is called statistical mechanics. One of the simplest such models is the Ising model [3] which is a model of a magnet. Traditionally, two-dimensional lattice models are studied by using transfer matrices. Lattice models are integrable (exactly solvable) when their transfer matrices satisfy the Yang-Baxter equation [5]. In this case the transfer matrices commute and this means that general Yang-Baxter techniques can be used to calculate many physical quantities of interest in the thermodynamic limit where the system size $N \rightarrow \infty$.

Conformal field theories were introduced in 1984 by Belavin, Polyakov and Zamolodchikov [7]. These theories describe the scaling limit of two-dimensional statistical systems at criticality. They can be classified by representations of the Virasoro algebra which is the algebra of conformal transformations of the plane into itself. The simplest family of such theories is the family of minimal models $\mathcal{M}(p, p')$ with p, p' coprime integers. These were also introduced by Belavin, Polyakov and Zamolodchikov [7]. The simplest among these describes the scaling limit of the two-dimensional Ising model [3] at criticality. In 1984, Friedan, Qiu and Shenker [8] classified the so-called *unitary* minimal models which describe the critical behaviour of the Andrews-Baxter-Forrester (ABF) Restricted-Solid-on-Solid (RSOS) models [9] which were also introduced in 1984. The ABF models generalize the Ising model and have the property that all of the Boltzmann weights are nonnegative. For the unitary models $p = p' - 1$. In this thesis, we consider the more general RSOS models of Forrester and Baxter [10] where $1 \leq p < p'$.

Corner Transfer Matrices were introduced by Baxter [5] to calculate the local height probabilities for sites deep in the lattice. The important ingredients in these calculations are the local height energies and the one-dimensional configurational sums. In Chapter 1 of this thesis we find a set of local heights that appears to be an alternative to the Forrester-Baxter local height energies. It is dependent on the banding structure introduced by Foda and Welsh [24].

Forrester and Baxter's calculations of the local height probabilities led to generalisations of the Rogers-Schur-Ramanujan identities [1],[2]. Moreover, the limit as $N \rightarrow \infty$ of the one-dimensional configurational sums coincide with the conformal characters [11] of the minimal models. These characters have two other forms of interest. The bosonic form of the characters is known as the Rocha-Caridi form [11]. The fermionic form is more complex; its fundamental form was first found by the Stony Brook group [16, 17, 15, 18] and further studied by Foda and Welsh [24]. Both of these forms for the characters can be finitised which is the suitable form for comparison to finite lattice results. The finitised fermionic

forms contain information on the particle content of the theories which is encoded in the (\mathbf{m}, \mathbf{n}) systems. The finitised characters reproduce the full conformal characters in the limit $N \rightarrow \infty$. The properties of finitised characters are discussed in Chapter 2.

Remarkably, the finitised characters also appear as the generating functions for the eigenenergies of the transfer matrices. In Chapter 3, we obtain these finitised characters from a combinatorial study of the eigenvalues of the transfer matrices. More specifically, for a number of typical examples, we compare path diagrams of the local heights with the zeros of the eigenvalues of the fused transfer matrices of the FB lattice models. We observe a relation between the features on the path and the patterns of the zeros. This leads us to a combinatorial interpretation of the (\mathbf{m}, \mathbf{n}) system and the particle content at least in the examples considered. This interpretation is called *physical combinatorics*.

In summary, this thesis is an exploration of the feasibility of describing the finitised characters of minimal models in terms of the *physical combinatorics* of patterns of zeros of the eigenvalues of the transfer matrices of the related lattice models.

Chapter 1

Forrester-Baxter Lattice Models

1.1 Boltzmann Weights and Local Properties

The Forrester-Baxter lattice models are Restricted Solid-on-Solid (RSOS) models on the square lattice. They are defined by associating to each lattice site a positive integer “height” $l_i = 1, 2, 3, \dots, p' - 1$. These heights are subject to the solid-on-solid restriction $|l_i - l_j| = 1$ where i and j are nearest-neighbour sites. The statistical behaviour of these models is determined by specifying Boltzmann weights for the elementary square faces

$$W\left(\begin{array}{c|c} d & c \\ a & b \end{array} \middle| u\right) \quad (1.1.1)$$

These give the *a priori* probability of finding a face in a given configuration. Here we have allowed for a dependence on a *spectral parameter* u , which is related to the spatial anisotropy. The statistical behaviour of the model is obtained by calculating the partition function

$$Z = \sum_{\text{heights}} \prod_{\text{faces}} W\left(\begin{array}{c|c} d & c \\ a & b \end{array} \middle| u\right) \quad (1.1.2)$$

1.1.1 Boltzmann weights

Let p and p' be two coprime positive integers with $1 \leq p \leq p' - 1$ and define the crossing parameter

$$\lambda = \frac{p' - p}{p'} \pi \quad (1.1.3)$$

The Boltzmann weights of the Forrester-Baxter models are then given explicitly by

$$W\left(\begin{array}{c|c} a \pm 1 & a \\ a & a \mp 1 \end{array} \middle| u\right) = \frac{s(\lambda - u)}{s(\lambda)} \quad (1.1.4)$$

$$W\left(\begin{array}{c|c} a & a \pm 1 \\ a \mp 1 & a \end{array} \middle| u\right) = \frac{g_{a \mp 1}}{g_{a \pm 1}} \left(\frac{s((a \pm 1)\lambda)}{s(a\lambda)} \right) \frac{s(u)}{s(\lambda)} \quad (1.1.5)$$

$$W\left(\begin{array}{c|c} a & a \pm 1 \\ a \pm 1 & a \end{array} \middle| u\right) = \frac{s(a\lambda \pm u)}{s(a\lambda)}. \quad (1.1.6)$$

Here $s(u) = \vartheta_1(u, \tilde{p})$ is a standard elliptic theta function

$$\vartheta_1(u, \tilde{p}) = 2\tilde{p}^{1/4} \sin u \prod_{n=1}^{\infty} (1 - 2\tilde{p}^{2n} \cos 2u + \tilde{p}^{4n})(1 - \tilde{p}^{2n}), \quad 0 \leq \tilde{p} \leq 1 \quad (1.1.7)$$

For $\tilde{p} = 0$ these models are *critical*. The elliptic nome $\tilde{p} \neq 0$ is a measure of the departure from criticality. The *gauge factors* g_a are arbitrary functions of a but we will take $g_a = 1$. With this choice the face weights are only invariant under reflections about one of the two diagonals. We will often call these models the $\mathcal{M}(p, p')$ models and refer to the model $\mathcal{M}(p' - p, p')$ as dual to the $\mathcal{M}(p, p')$ model.

The family of RSOS models with $p = p' - 1$ and $\lambda = \pi/p'$ were introduced by Andrews-Baxter-Forrester [9] before the Forrester-Baxter models. For this family of models, all of the Boltzmann weights are non-negative for $0 \leq u \leq \lambda$. This condition is consistent with the interpretation of the local Boltzmann weights as probabilities. In this case the models are called *unitary*. If $p \neq p' - 1$, some of the Boltzmann weights are negative. In this case, the models are called *non-unitary*.

The weights of the Forrester-Baxter models are \mathbb{Z}_2 symmetric under the height-reversal symmetry $a \mapsto p' - a$. This is the generic symmetry for these models except for the models $\mathcal{M}(1, p')$ with $p = 1$. In this case the models are in fact $\mathbb{Z}_{p'-2}$ parafermions which admit a $\mathbb{Z}_{p'-2}$ symmetry rather than a \mathbb{Z}_2 symmetry in the ground state. The unitary minimal models $\mathcal{M}(p' - 1, p')$ and $\mathbb{Z}_{p'-2}$ parafermions $\mathcal{M}(1, p')$ are dual models.

Later we will mostly be interested in the critical models. In this case, since we only have ratios of elliptic functions, the elliptic functions can be replaced by simple trigonometric functions

$$s(u) = \sin u \quad (1.1.8)$$

1.2 One-Dimensional Configurational Sums

1.2.1 Local height probabilities and one-dimensional sums

The local height probabilities P_a are fundamental physical properties of the off-critical RSOS models. These give the probability of finding a site deep in the lattice in the state a . These quantities were calculated using Corner Transfer Matrices (CTMs) by Forrester-Baxter [10].

The local height probabilities are defined by

$$P_{a'} = Z^{-1} \sum_{\text{heights}} \delta(a, a') \prod_{\text{faces}} W \left(\begin{matrix} d & c \\ a & b \end{matrix} \middle| u \right) \quad (1.2.1)$$

where Z is the partition function defined in 1.1.2 and δ is the Kronecker delta. The local height probability is the probability that a fixed site deep in the lattice has height $a = a'$. In taking the thermodynamic limit, the boundaries of the lattice are fixed. In general, the local height probabilities depend on the choice of boundary conditions. Depending on the model, there can be many different boundary conditions.

Here we are only concerned with regime III , where $0 < \tilde{p} < 1$ (\tilde{p} is the nome) and $0 < u < \lambda$. The result [10] for the local height probabilities in regime III is [10]

$$P_a = \frac{u_a X_N(a, b, c; x^t)}{\sum_{1 \leq a < p' - 1} u_a X_N(a, b, c; x^t)} \quad (1.2.2)$$

where u_a are certain functions which are not important for us and the *one-dimensional configurational sums* are the polynomials

$$X_N(a, b, c; q) = q^{-E_0} \sum_{l_2, l_3, \dots, l_{N-1}} q^{\sum_{j=1}^N j H(l_{j-1}, l_j, l_{j+1})} = \sum_l q^{E(l) - E_0} \quad (1.2.3)$$

Here the sum is over paths $l = \{l_1, l_2, l_3, \dots, l_N, l_{N+1}\}$ that label the entries of the CTMs. The paths are restricted such that $l_1 = a$, $|l_j - l_{j+1}| = 1$ and the boundary condition enters through $l_N = b$ and $l_{N+1} = c = b \pm 1$. The parameter q is related to the elliptic nome \tilde{p} . The functions $H(l_{j-1}, l_j, l_{j+1})$ give local energies associated with features in successive triplets of heights along the path and their sum is the energy of the path:

$$E(l) = \sum_{j=1}^N j H(l_{j-1}, l_j, l_{j+1}) \quad (1.2.4)$$

The energy E_0 is the energy of the groundstate path

$$E_0 = \min_l E(l) \quad (1.2.5)$$

This fixed energy cancels out of the local height probabilities but is convenient to ensure that the polynomials $X_N(a, b, c; q)$ begin as $X_N(a, b, c; q) = 1 + O(q)$. Observe that by the RSOS restriction we must have $N = a - b \bmod 2$ where N is the system size.

The explicit expressions for the local energies obtained by Forrester-Baxter [10] are

$$H(l, l-1, l) = \left\lfloor \frac{l(p' - p)}{p'} \right\rfloor \quad (1.2.6)$$

$$H(l, l+1, l) = -\left\lfloor \frac{l(p' - p)}{p'} \right\rfloor \quad (1.2.7)$$

$$H(l-1, l, l+1) = H(l+1, l, l-1) = \frac{1}{2} \quad (1.2.8)$$

Consider an example of the local energies of a path $l = \{1, 2, 1, 2, 3, 4, 3, 2, 1\}$ for $\mathcal{M}(3, 5)$. In this example, $E_0 = 0$ and the total energy of the path is

$$\begin{aligned} E(l) &= H(1, 2, 1) + 2H(2, 1, 2) + 3H(1, 2, 3) + 4H(2, 3, 4) + 5H(3, 4, 3) \\ &\quad + 6H(4, 3, 2) + 7H(3, 2, 1) \\ &= 0 + 0 + 3\frac{1}{2} + 4\frac{1}{2} + 5(-1) + 6\frac{1}{2} + 7\frac{1}{2} = 5 \end{aligned}$$

There are many possible paths for $\mathcal{M}(3, 5)$ with $(a, b, c) = (1, 1, 2)$ and $N = 8$. The total energies E appear as the exponents in the one-dimensional configurational sum for the given

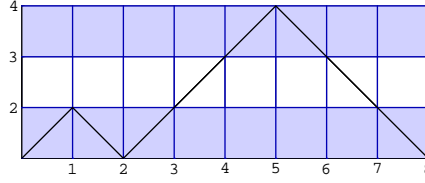


Figure 1.1: One of the paths for $\mathcal{M}(3,5)$ with $N = 8$ and energy = 5. The shading of the rows is explained in the next section.

boundary conditions and system size. To construct the whole sum $X_N(a, b, c; q)$, we need to sum the total energies of each of the possible paths:

$$X_8(1, 1, 2; q) = 1 + q^2 + q^3 + 2q^4 + q^5 + 2q^6 + q^7 + q^8 + q^9 + q^{10} + q^{12} \quad (1.2.9)$$

Degeneracies appear as coefficients in front of the powers. Replacing q with 1, $X_N(a, b, c; 1)$ gives the number of paths from a to b in N steps. Notice that the example path above is the only one of energy $E = 5$.

Generally, the number of paths from height a to height b in N steps is

$$(A^N)_{a,b} = X_N(a, b, b \pm 1; 1) = \{\# \text{ of paths from } a \text{ to } b \text{ in } N \text{ steps}\} \quad (1.2.10)$$

where A is the adjacency matrix encoding the allowed heights for neighbouring sites on the path. For example, the adjacency matrix for a model with $p' = 5$ is

$$\begin{pmatrix} 0 & 1 & 0 & 0 \\ 1 & 0 & 1 & 0 \\ 0 & 1 & 0 & 1 \\ 0 & 0 & 1 & 0 \end{pmatrix} \quad (1.2.11)$$

This shows that height 1 can connect to height 2 only, height 2 can connect to heights 3 and 1 and so on.

The one-dimensional configurational sums will reappear in a different context in the study of the physical combinatorics of these models at criticality.

1.2.2 Alternate local energies

The form of the local energies $H(l_{j-1}, l_j, l_{j+1})$ are not unique. Here we look for a simpler alternative form for these local energies. The Forrester-Baxter form involves floor functions and terms are of both signs. We have demonstrated, at least for relatively small p and p' , that a simpler alternative $H'(l_{j-1}, l_j, l_{j+1})$ exists which only involves non-negative weights $0, \frac{1}{4}, \frac{1}{2}, 1$ and no floor functions. As a bonus, unlike the Forrester-Baxter form, the alternative form is \mathbb{Z}_2 symmetric under height reversal $l \leftrightarrow p' - l$. As we will explain later we believe, at least at criticality, that this form will be more closely related to the particle content of the theory and in this sense is more physical.

The dependence of H' on features of the path is more complex than that of H . In particular, the method depends on the *banding structure* of the models. We now introduce the banding structure following Foda & Welsh [24].

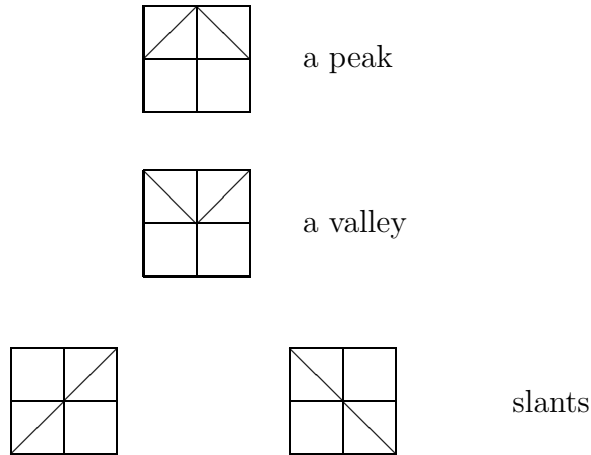
Banding structure

In order to define the new rules for local energies, we first introduce a ‘banding structure’ for the path diagrams. The l -th band is the horizontal strip between two successive heights l and $l + 1$ on the path. In this banding structure, each band is given a parity: the l -th band is *even* if $\lfloor \frac{lp}{p'} \rfloor = \lfloor \frac{(l+1)p}{p'} \rfloor$, and it is *odd* if $\lfloor \frac{lp}{p'} \rfloor \neq \lfloor \frac{(l+1)p}{p'} \rfloor$. For all models there are $p' - 2$ bands, of which $p' - p - 1$ are even bands and $p - 1$ are odd. For p and p' co-prime, the banding is always symmetrical about the centre (either the centre band or centre height). By convention, the odd bands are shaded. The height of the lower edge of the n -th odd band (not the n -th band) is $\lfloor \frac{np'}{p} \rfloor$. Equivalently, the height of the upper edge of the n -th odd band is $\lceil \frac{np'}{p} \rceil$.

The banding structure of the path diagrams for the dual model $\mathcal{M}(p' - p, p')$ is the reverse of that for the path diagrams of $\mathcal{M}(p, p')$. These models have the same number of bands, and each band that was even in $\mathcal{M}(p, p')$ is odd in the dual $\mathcal{M}(p' - p, p')$ and vice versa. This follows because, for p and p' coprime, the statements $\lfloor \frac{lp}{p'} \rfloor = \lfloor \frac{(l+1)p}{p'} \rfloor$ and $\lfloor \frac{l(p'-p)}{p'} \rfloor \neq \lfloor \frac{(l+1)(p'-p)}{p'} \rfloor$ are equivalent for bands labelled by $l = 1, 2, \dots, p' - 2$.

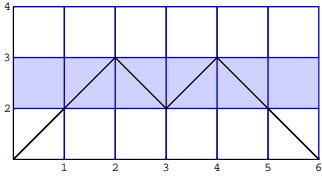
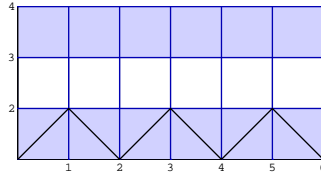
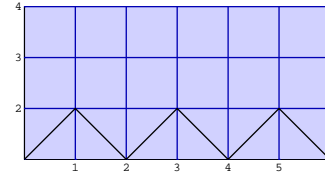
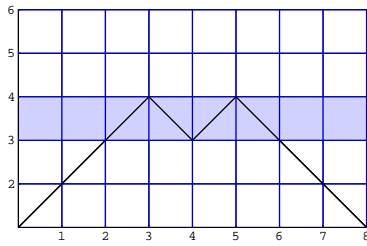
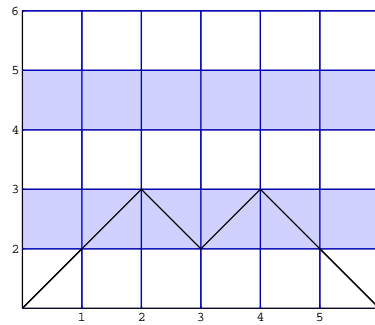
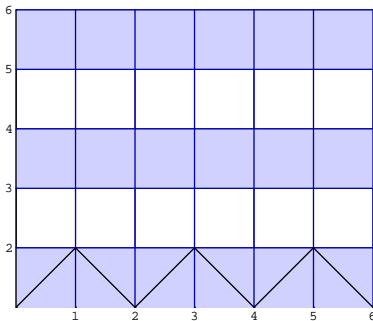
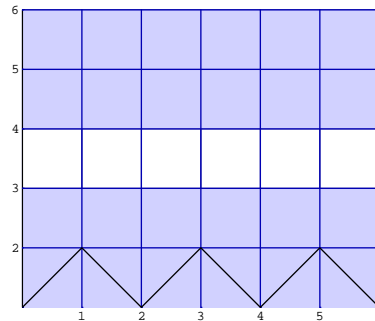
The local energy function H'

The local energies H' depend on the local shape of the path. Locally, the path can have either a local maximum, a local minimum or it can be increasing or decreasing. We call these local shapes respectively peaks, valleys, (increasing) slants and (decreasing) slants



Generally, the local energies favour (assign lower energies to) slants in the unshaded regions and favour the peaks and valleys in the shaded regions. We will always assign the two orientations of slants at the same height the same weight. In specifying the weights, we break the path diagrams down into three regions, namely the *outside*, the *inside* and the *centre*, according to its band structure; different regions have different weighting rules for H' . Not all of the regions are present in all models. There is firstly a special weight assigned for features in odd bands, and this holds across all regions. If there are two contiguous odd bands, slants across these two bands have weight $\frac{1}{2}$. This is the only instance in which

Illustration of the banding structure for some $\mathcal{M}(p, p')$ models. The particular path shown is the ground state, that is, the path with lowest energy.

Figure 1.2: $\mathcal{M}(2, 5)$ Figure 1.3: $\mathcal{M}(3, 5)$ Figure 1.4: $\mathcal{M}(4, 5)$ Figure 1.5: $\mathcal{M}(2, 7)$ Figure 1.6: $\mathcal{M}(3, 7)$ Figure 1.7: $\mathcal{M}(4, 7)$ Figure 1.8: $\mathcal{M}(5, 7)$

features occurring entirely within odd bands have nonzero weight. Slants that cross from an odd band to an even band, or from an even band to an odd band may have nonzero weight.

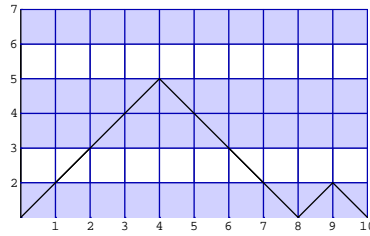


Figure 1.9: The slants at 3 and 5 are each weighted $\frac{1}{2}$ as they cross contiguous odd bands. At 1,2,6 & 7 there are slants crossing an odd band and a single even band. These may also have nonzero weights.

The outside region

The assignment of weights is the simplest for the outside region. We divide the outside region into two regions. The *upper outside* region denotes the even bands that are above the highest odd (shaded) band. The *lower outside* region denotes the even bands below the lowest odd (shaded) band. In the upper outside region, peaks have weight one and valleys have weight zero. In the lower outside region, valleys have weight one and peaks have weight zero. Notice that $\mathcal{M}(5, 8)$, for example, has no outside region since it has an odd first and

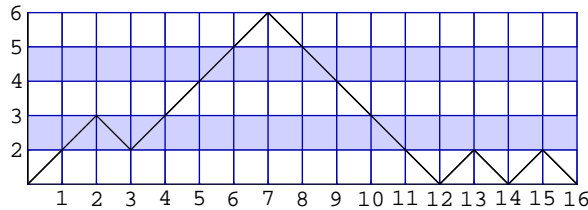


Figure 1.10: The peak at 7 and the valleys at 12 and 14 all have weight 1 by the above rules.

last (6th) band and therefore there are no even bands above the highest odd band or below the lowest odd band.

The centre region

The *centre* region consists of a number of bands about the centre band or height. The bands that are included in this region vary. The banding structure for the centre region has four cases, differentiated by the number and parity of centre bands. These cases are p' odd and p even, p' odd and p odd, p' even and p odd with odd centre bands and with even centre bands. These four cases are illustrated in 1.11,1.12,1.2.2,1.2.2.

(i) Models with an odd number of bands (p' odd) have a single centre band at $j = (p' - 1)/2$.

If p is odd, these models have an even centre band. The centre region then consists of just this single band. Peaks and valleys in this even centre band are weighted $\frac{1}{2}$. Slants

across this centre band that cross to either the band above or the band below are weighted $\frac{1}{4}$. This combination of weights, $\frac{1}{4}$ for slants and $\frac{1}{2}$ for peaks and valleys in a even band, is a feature of weights in the centre region.

If p is even, these models have an odd centre band. The centre region then consists of all of the bands around the centre, up to and including the first even bands encountered. Shapes in these even bands immediately above and below the odd centre band have nonzero weights. The weights are as for in the centre band above; slants that cross the band are weighted $\frac{1}{4}$ and peaks and valleys in the band are weighted $\frac{1}{2}$. Slants in contiguous odd bands have as usual weight $\frac{1}{2}$.

(ii) Models with an even number of bands (p' even) have a central height at $j = p'/2$. The bands immediately above and below the central height are the bands at $p'/2 - 1$ and at $p'/2$. We call these the *centre two bands*. The centre two bands have the same parity.

If the centre two bands are even, they constitute the *centre region*. Slants ‘across the centre’ refers to slants that cross from one of the centre two bands to the other. Slants across the centre have weight $\frac{1}{2}$. Peaks on the lower band and valleys on the upper band have weights of 1.

If the centre two bands are odd, the centre region consists of all of the bands around the centre, up to and including the first even bands encountered. The two odd bands are weighted as for contiguous odd bands everywhere; slants across the centre have weight $\frac{1}{2}$.

Elsewhere in the centre region all weights are zero.

The inside region

The *inside* region is all of the bands that are not in the centre or outside region. We denote all of the bands above the centre region and below the upper outside region as the *upper inside region*, and all of the bands below the centre region and above the lower outside region as the *lower inside region*. All shapes in single even bands in the inside region are weighted as for shapes in single even centre bands, that is, $\frac{1}{4}$ for slants and $\frac{1}{4}$ for peaks and valleys. Here slants includes all slants that cross into or out of this band in either direction. All peaks in (not single) even bands in the lower inside region have a weight of 1. Valleys in (not single) even bands in the upper inside region have weight 1.

An example weighted path

Here is an example of calculating the weight of a path for $\mathcal{M}(4,9)$ and $a = b = 1$. The outside region of this path diagram consists of bands 1 and 7. There is a valley in band 1 at step $j = 14$, with weight 1. The centre region $j = 3, 4, 5$ consists of the odd centre band ($j = 4$) and the adjacent bands $j = 3, 5$. Path shapes have non-zero weights in the even bands 3 and 5. In band 3 there are slants crossing it at steps $j = 2, 5, 11, 12$, all with weight $\frac{1}{4}$. There is also a peak at step $j = 3$ and a valley at step $j = 4$, both with weight $\frac{1}{2}$. In band 5 there are slants at steps $j = 6, 7, 9, 10$, all with weight $\frac{1}{4}$. The inside region consists of bands $j = 2, 6$. These are single odd bands so the shapes in this region have weight 0.

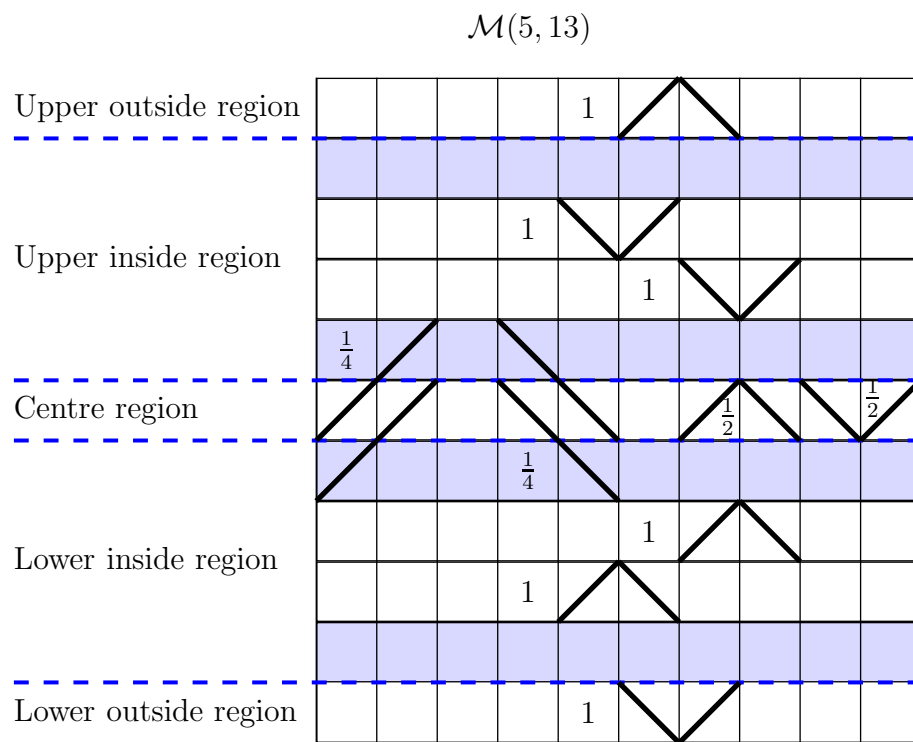


Figure 1.11: Illustration of the weighting rules for a case p' odd, p odd

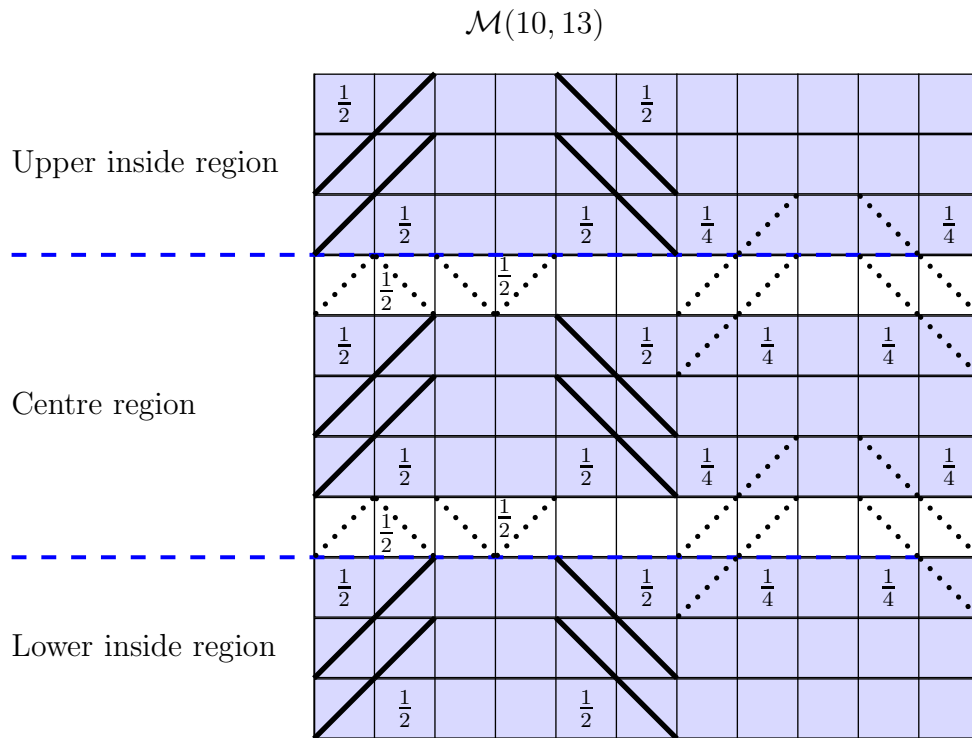


Figure 1.12: Illustration of the weighting rules for a case p' odd, p even. The dotted lines indicate the features with nonzero weights in the 'centre two band'.

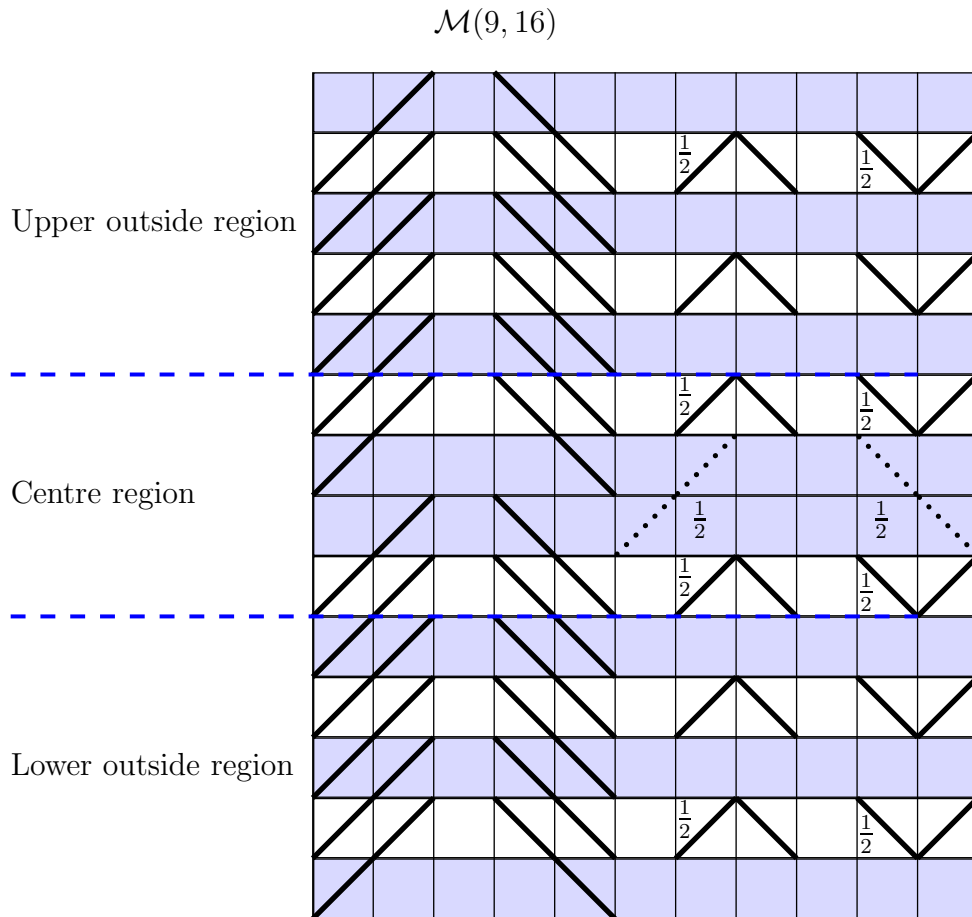
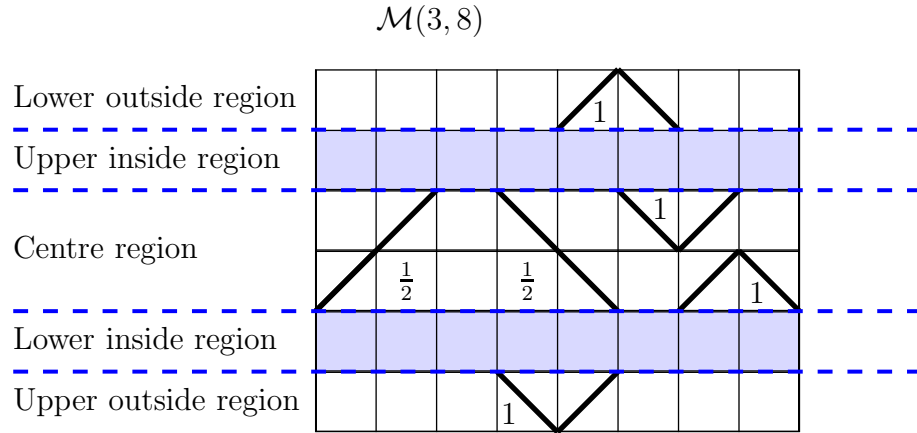
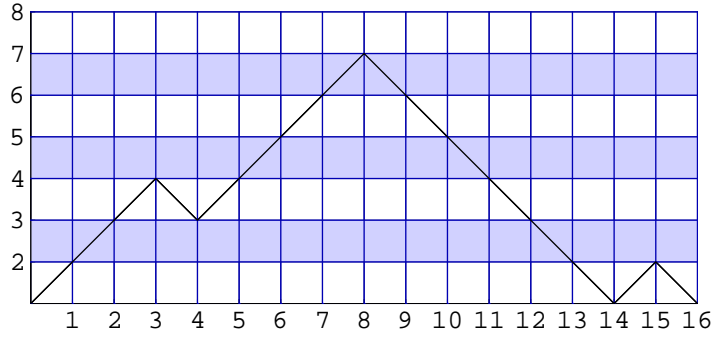


Figure 1.13: Illustration of the weighting rules for a case p' even, centre two band odd. The dotted lines show slants in contiguous odd bands, which have the same weight in all regions. All other slants in the above diagram have weight $\frac{1}{4}$.

Figure 1.14: Illustration of the weighting rules for a case p' even, centre two band evenFigure 1.15: A path in $\mathcal{M}(4, 9)$ with $N = 16$.

The total energy of this path is

$$\begin{aligned}
 E(l) &= H'(1, 2, 1) + 2H'(2, 3, 4) + 3H'(3, 4, 3) + 4H'(4, 3, 4) + 5H'(3, 4, 5) + 6H'(4, 5, 6) \\
 &\quad + 7H'(5, 6, 7) + 8H'(6, 7, 6) + 9H'(7, 6, 5) + 10H'(6, 5, 4) + 11H'(5, 4, 3) \\
 &\quad + 12H'(4, 3, 2) + 13H'(3, 2, 1) + 14H'(2, 1, 2) + 15H'(1, 2, 1) \tag{1.2.12} \\
 &= 0 + 2\frac{1}{4} + 3\frac{1}{2} + 4\frac{1}{2} + 5\frac{1}{4} + 6\frac{1}{4} + 7\frac{1}{4} + 0 + 9\frac{1}{4} + 10\frac{1}{4} + 11\frac{1}{4} + 12\frac{1}{4} + 0 + 14 + 0 \\
 &= 33
 \end{aligned}$$

This agrees with the total energy obtained from the Forrester-Baxter local energies for the same path

$$E(l) = \sum_{j=1}^N jH(l_{j-1}, l_j, l_{j+1}) = 33 \tag{1.2.13}$$

We stress that the local energies H' are \mathbb{Z}_2 symmetric. This can be seen from the symmetry of the weighting rules and through their dependence on the path structure. Every feature in the upper or lower half of the path diagram that is given a non-zero weight by

the rules in H' has a corresponding feature in the other half that is its reflection and has the same weight. The combination of $\frac{1}{4}, \frac{1}{4}, \frac{1}{2}, \frac{1}{2}$ for slants of both kinds, peaks and valleys respectively in the centre region and single even bands is constructed to have \mathbb{Z}_2 symmetry.

In the example above, if the path is reflected about the centre, then the path starts and ends at $a = b = 8$ and the peak in the 6th band becomes a valley in the second band. The tip of the peak in band 6 is at height 7, so the bottom of the valley would be at height $p' - 7 = 2$. Calculating the energy in exactly the same way as above on this inverted path gives the same result.

Some one-dimensional configurational sums

The one-dimensional configurational sums $X_N(a, b, c; q)$ for given p, p' and system size N are obtained by summing the monomials q^{E-E_0} over the total energies E of all paths subject to the given boundary conditions specified by a, b, c . Increasing the system size N increases the order of the polynomial $X_N(a, b, c; q)$. The coefficients of a fixed power of q settles eventually to a constant as N is increased. We demonstrate this with the example of $\mathcal{M}(2, 7)$ with $a = b = 1$ and $E_0 = 0$. For $N = 4, 6, 8, \dots$

$$\begin{aligned}
X_4(1, 1, 2; q) &= 1 + q^2 \\
X_6(1, 1, 2; q) &= 1 + q^2 + q^3 + q^4 + q^5 + q^6 \\
X_8(1, 1, 2; q) &= 1 + q^2 + q^3 + 2q^4 + q^5 + 2q^6 + q^7 + 2q^8 + q^{10} + q^{12} \\
X_{10}(1, 1, 2; q) &= 1 + q^2 + q^3 + 2q^4 + 2q^5 + 3q^6 + 2q^7 + 4q^8 + 3q^9 + 4q^{10} \\
&\quad + 3q^{11} + 4q^{12} + 3q^{14} + 2q^{15} + 2q^{16} + q^{17} + q^{18} + q^{20} \quad (1.2.14) \\
X_{12}(1, 1, 2; q) &= 1 + q^2 + q^3 + 2q^4 + 2q^5 + 3q^6 + 3q^7 + 5q^8 + 5q^9 + 7q^{10} + 6q^{11} \\
&\quad + 9q^{12} + 7q^{13} + 9q^{14} + 8q^{15} + 9q^{16} + 7q^{17} + 9q^{18} + 6q^{19} + 7q^{20} \\
&\quad + 5q^{21} + 5q^{22} + 3q^{23} + 4q^{24} + 2q^{25} + 2q^{26} + q^{27} + q^{28} + q^{30}
\end{aligned}$$

We see that the coefficients of q^1, q^2, q^3 do not change with N . The coefficients of q^4 and q^5 appear to have stopped increasing from $N > 8$ and $N > 10$ respectively, and in fact they do remain constant for all greater values of N . The lower energy paths are present even for small system sizes; $N = 4$ for $\mathcal{M}(2, 7)$ is a sufficient size to contain all possible paths of energy 2, and the coefficient of q^2 will not increase with N . However, system size $N = 8$ is not of a sufficient size to contain one of the two paths of energy 5. As the system size grows, all paths of a fixed energy will appear. In the limit as $N \rightarrow \infty$, all paths of all allowed energies will be present, and the one-dimensional configurational sum will be a fixed ‘infinite polynomial’ in q .

1.3 Double-Row Transfer Matrices

We are interested in studying the critical Baxter-Forrester lattice models on a finite width strip with specified boundary conditions on the left and the right boundaries. To do this we need to introduce double row transfer matrices.

For a lattice of width N , the entries of $\mathbf{D}(u)$ are given diagrammatically by

$$\mathbf{D}(u)_{a,b} = \sum_{c_0, \dots, c_N} \lambda \begin{array}{c} \begin{array}{ccccccc} a & a & b_1 & b_2 & & b_{N-1} & b & b \\ \begin{array}{c} \diagdown \\ \diagup \end{array} & \begin{array}{|c|c|c|c|} \hline \lambda-u & \lambda-u & & \lambda-u \\ \hline \end{array} & \begin{array}{c} \diagup \\ \diagdown \end{array} \\ \hline c_0 & c_1 & c_2 & & c_{N-1} & c_N \\ \hline u & u & & u & \\ \hline a & a_1 & a_2 & & a_{N-1} & b & b \\ \begin{array}{c} \diagup \\ \diagdown \end{array} & & & & & \begin{array}{c} \diagdown \\ \diagup \end{array} \\ \hline \end{array} \end{array} \quad (1.3.1)$$

For given boundary conditions, the partition function for a strip with N columns and M double rows is then given by

$$Z = \text{Tr } \mathbf{D}(u)^N \quad (1.3.2)$$

The boundary triangles are added to ensure integrability of the lattice model in the presence of a boundary [21]. In this context, integrability in the sense of Yang-Baxter is equivalent to requiring commuting double row transfer matrices. To achieve this the local face weights and boundary triangle weights must satisfy the bulk Yang-Baxter equations (YBE)

$$\sum_g W \left(\begin{array}{c|c} g & d \\ b & c \end{array} \middle| u \right) W \left(\begin{array}{c|c} f & e \\ g & d \end{array} \middle| v \right) W \left(\begin{array}{c|c} f & g \\ a & b \end{array} \middle| u-v \right) = \sum_g W \left(\begin{array}{c|c} f & e \\ a & g \end{array} \middle| u \right) W \left(\begin{array}{c|c} a & g \\ b & c \end{array} \middle| v \right) W \left(\begin{array}{c|c} e & d \\ g & c \end{array} \middle| u-v \right) \quad (1.3.3)$$

and the boundary Yang-Baxter equations (BYBEs)

$$\begin{aligned} & \sum_{f,g} W \left(\begin{array}{c|c} c & f \\ b & a \end{array} \middle| u-v \right) W \left(\begin{array}{c|c} d & g \\ c & f \end{array} \middle| \lambda-u-v \right) K_R \left(\begin{array}{c|c} f & g \\ a & u \end{array} \right) K_R \left(\begin{array}{c|c} d & e \\ g & v \end{array} \right) \\ & = \sum_{f,g} W \left(\begin{array}{c|c} e & f \\ d & c \end{array} \middle| u-v \right) W \left(\begin{array}{c|c} f & g \\ c & b \end{array} \middle| \lambda-u-v \right) K_R \left(\begin{array}{c|c} b & g \\ a & v \end{array} \right) K_R \left(\begin{array}{c|c} f & e \\ g & u \end{array} \right) \end{aligned} \quad (1.3.4)$$

There are many solutions of the boundary Yang-Baxter equations corresponding to many different integrable boundary conditions. These are usually labelled [23] by a pair of positive integers (r, s) . In this case the rows and columns of the double row transfer matrix are labelled by the paths from height $s = a$ to height b in N steps. Later, when we relate the eigenvalue spectra of the double row transfer matrices to the one-dimensional configurational sums, the boundary condition labels r, s will be simply related to the labels a, b, c of the one-dimensional configurational sums by $a = s$, $b = b(r) = \lfloor \frac{rp'}{p} \rfloor$ and $c = b \pm 1$ where $a = ss = 1, 2, \dots, p' - 1$ and $b = 1, 2, \dots, p - 1$.

The simplest solution to the BYBE is the so-called *vacuum* solution. For this solution the boundary weights are given by

$$K_R \left(\begin{array}{c|c} 1 & 1 \\ 2 & 1 \end{array} \middle| u \right) = 1, \quad K_R \left(\begin{array}{c|c} c & b \\ c & b \end{array} \middle| u \right) = 0, \quad (b, c) \neq (1, 2) \quad (1.3.5)$$

We will only consider this solution.

The local YBEs and BYBEs suffice to guarantee commuting transfer matrices [21]. Also the double row transfer matrices are positive definite and satisfy crossing symmetry $\mathbf{D}(u) = \mathbf{D}(\lambda - u)$.

Chapter 2

Conformal Field Theory

2.1 Minimal Models

The continuum scaling limits of critical lattice models, where $N \rightarrow \infty$ and the discrete lattice spacing $\delta \rightarrow 0$ with $N\delta \rightarrow R$ a continuum coordinate, are associated with continuum theories. These theories are invariant under conformal transformations of the plane into itself and so are called *Conformal Field Theories* (CFTs). CFTs are *universal* in the sense that they do not depend on the detailed structure of the lattice, for example, square versus triangular lattice. The CFTs obtained from the continuum scaling limit of the Forrester-Baxter models are the *Minimal Models*. These are comparatively simple conformal field theories that describe discrete statistical models at their critical points.

Conformal field theories are characterised in terms of a set of conformal data which includes the central charge c , a set of conformal weights Δ and their associated characters. We will now describe this data for the minimal models.

Minimal models $\mathcal{M}(p, p')$ [7], where \mathcal{M} stands for minimal, are characterised by a central charge c

$$c = 1 - \frac{6(p - p')^2}{pp'}, \quad 1 < p < p' \quad (2.1.1)$$

where p and p' are relatively prime positive integers with $p < p'$ exactly as in the Forrester-Baxter models. The $\mathcal{M}(1, p')$ models are not minimal models. By convention we identify the $\mathcal{M}(1, p')$ models with the $\mathbb{Z}_{p'-2}$ parafermions. These models have a different symmetry to the minimal models and are in a different universality class with central charges

$$c = \frac{2(p' - 3)}{p'}, \quad (2.1.2)$$

Values of the central charge for some models are shown in the Table.

The critical exponents of lattice models are related to the conformal weights of the associated CFT. The minimal models have conformal weights

$$\Delta_{r,s}^{(p,p')} = \frac{(rp' - sp)^2 - (p - p')^2}{4pp'}, \quad 1 \leq r \leq p - 1, \quad 1 \leq s \leq p' - 1 \quad (2.1.3)$$

Each conformal weight is associated with an operator or field in the CFT. For example, the three conformal weights of the Ising model are associated with the identity ($\Delta = 0$), the

Name	Model	Central Charge c
Ising	$\mathcal{M}(3, 4) \equiv \mathcal{M}(1, 4)$	$\frac{1}{2}$
Hard Hexagons	$\mathcal{M}(1, 5)$	$\frac{4}{5}$
Tricritical Ising	$\mathcal{M}(4, 5)$	$\frac{7}{10}$
Yang-Lee	$\mathcal{M}(2, 5)$	$-\frac{22}{5}$
	$\mathcal{M}(3, 5)$	$-\frac{3}{5}$
	$\mathcal{M}(2, 7)$	$-\frac{68}{7}$
	$\mathcal{M}(3, 7)$	$-\frac{25}{7}$
	$\mathcal{M}(4, 7)$	$-\frac{13}{14}$
	$\mathcal{M}(5, 7)$	$\frac{11}{35}$

magnetization ($\Delta = 1/16$) and the energy ($\Delta = 1/2$). The *Kac table* of an $\mathcal{M}(p, p')$ model is the grid of conformal weights for all allowed values of r, s . In the Figure are the Kac tables for the minimal models listed in the previous Table. The conformal weights have the symmetry $\Delta_{r,s} = \Delta_{p-r, p'-s}$. This means that each entry occurs twice in the Kac table; half of the values are redundant.

Conformal field theories are classified into *unitary* and *non-unitary* theories. If a CFT is *unitary*, all of the conformal weights are non-negative. If there are some negative conformal weights then the theory is non-unitary. In the case of minimal models, the theories $\mathcal{M}(p, p')$ with $p = p' - 1$ are unitary whereas the models with $2 \leq p \leq p' - 2$ and $p' \geq 4$ are non-unitary. This is in accord with the conformal weights shown in the above Kac tables. In what follows we will mostly be concerned with the non-unitary models.

2.2 Bosonic Characters

To each operator in a CFT there is an associated conformal weight Δ and a conformal character $\chi_\Delta(q)$. The character is the generating function for the spectra of the theory on a strip with boundary conditions conjugate to the given operator. For the minimal models, the operators and their conjugate boundary conditions are labelled by r and s as in the Kac tables. The conformal characters of the minimal models are [11]

$$\chi_{r,s}^{(p,p')}(q) = q^{\Delta_{r,s}^{(p,p')}-c/24} B_{r,s}(q) \quad (2.2.1)$$

where

$$B_{r,s}(q) = \frac{1}{(q)_\infty} \sum_{j=-\infty}^{\infty} (q^{j(pp'+rp'-sp)} - q^{(jp'+s)(jp+r)}) \quad (2.2.2)$$

and

$$(q)_n = \prod_{j=1}^n (1 - q^j), \quad (q)_0 = 1, \quad (q)_\infty = \prod_{j=1}^{\infty} (1 - q^j) \quad (2.2.3)$$

$\mathcal{M}(3, 4)$

s		
3	$\frac{1}{2}$	0
2	$\frac{1}{16}$	$\frac{1}{16}$
1	0	$\frac{1}{2}$
	r	1 2

$\mathcal{M}(2, 5)$

s	
4	0
3	$-\frac{1}{5}$
2	$-\frac{1}{5}$
1	0
	r

$\mathcal{M}(2, 7)$

s	
6	0
5	$-\frac{2}{7}$
4	$-\frac{3}{7}$
3	$-\frac{3}{7}$
2	$-\frac{2}{7}$
1	0
	r

$\mathcal{M}(4, 7)$

s			
6	$\frac{5}{2}$	$\frac{13}{16}$	0
5	$\frac{10}{7}$	$\frac{27}{112}$	$-\frac{1}{14}$
4	$\frac{9}{14}$	$-\frac{5}{112}$	$\frac{1}{7}$
3	$\frac{1}{7}$	$-\frac{5}{112}$	$\frac{9}{14}$
2	$-\frac{1}{14}$	$\frac{27}{112}$	$\frac{10}{7}$
1	0	$\frac{13}{16}$	$\frac{5}{2}$
	r	3 2 1	

$\mathcal{M}(4, 5)$

s			
4	$\frac{3}{2}$	$\frac{7}{16}$	0
3	$\frac{3}{5}$	$\frac{3}{80}$	$\frac{1}{10}$
2	$\frac{1}{10}$	$\frac{3}{80}$	$\frac{3}{5}$
1	0	$\frac{7}{16}$	$\frac{3}{2}$
	r	1 2 3	

$\mathcal{M}(3, 5)$

s	
4	$\frac{3}{4}$
3	$\frac{1}{5}$
2	$-\frac{1}{20}$
1	0
	r

$\mathcal{M}(3, 7)$

s	
6	$\frac{5}{4}$
5	$\frac{4}{7}$
4	$\frac{3}{28}$
3	$-\frac{1}{7}$
2	$-\frac{5}{28}$
1	0
	r

$\mathcal{M}(5, 7)$

s				
6	$\frac{15}{4}$	$\frac{9}{5}$	$\frac{11}{20}$	0
5	$\frac{16}{7}$	$\frac{117}{140}$	$\frac{3}{35}$	$\frac{1}{28}$
4	$\frac{33}{28}$	$\frac{8}{35}$	$-\frac{3}{140}$	$\frac{3}{7}$
3	$\frac{3}{7}$	$-\frac{3}{140}$	$\frac{8}{35}$	$\frac{33}{28}$
2	$\frac{1}{28}$	$\frac{3}{35}$	$\frac{117}{140}$	$\frac{16}{7}$
1	0	$\frac{11}{20}$	$\frac{9}{5}$	$\frac{15}{4}$
	r	1 2 3 4		

In fact there are several different forms for these characters. The above expressions have coefficients of both signs, and are consequently called *bosonic*. This is in distinction to *fermionic* expressions which have only positive coefficients. There are at least three distinct forms for the minimal model characters. The second form is the *fermionic* form which has all positive coefficients and is structured by information related to the particle content and encoded in the so-called (\mathbf{m}, \mathbf{n}) system which we will explain later. It turns out that the third form is given by the limit as $N \rightarrow \infty$ of the one-dimensional configurational sums of Chapter 2. These forms have all positive coefficients but they are *not* referred to as fermionic since the polynomials are unstructured. We will now look more closely at the fermionic forms for the characters of the minimal models. These admit a finitised form that contains information on a finite lattice, and is dependent on system size N . The full conformal characters are then obtained by taking the limit $N \rightarrow \infty$.

2.3 Finitised Characters

In order to describe (\mathbf{m}, \mathbf{n}) systems and the associated finitised characters, we first need to introduce the continued fraction decomposition of p'/p .

2.3.1 Continued fraction decomposition

Consider the minimal model $\mathcal{M}(p, p')$ with $2 < 2p < p'$. In this case the fraction p'/p admits a continued fraction decomposition of the following form

$$\frac{p'}{p} = \nu_0 + 1 + \frac{1}{\nu_1 + \frac{1}{\nu_2 + \dots + \frac{1}{\nu_n + 2}}} \quad (2.3.1)$$

where $\nu_0 > 0$ and $\nu_j \geq 1$ for $j = 1, 2, \dots, n$. The number ν_j is the number of types of quasi-particles in zone j . There are $n+1$ zones. If $2p > p'$, one simply replaces p with $p' - p$ as for the dual and then carry out the continued fraction decomposition. We will refer to

$$t = t_{n+1} = \sum_{j=0}^n \nu_j \quad (2.3.2)$$

as the total number of types of *quasi-particles*. Here is a table of values of t with the rows labelled by $p = 1, 2, \dots, 8$ and columns labelled by $p' = 4, 5, \dots, 10$:

$$\begin{pmatrix} 1 & 2 & 3 & 4 & 5 & 6 & 7 \\ 0 & 1 & 0 & 2 & 0 & 3 & 0 \\ 1 & 1 & 0 & 2 & 2 & 0 & 3 \\ 0 & 2 & 0 & 2 & 0 & 3 & 0 \\ 0 & 0 & 3 & 2 & 2 & 3 & 0 \\ 0 & 0 & 0 & 4 & 0 & 0 & 0 \\ 0 & 0 & 0 & 0 & 5 & 3 & 3 \\ 0 & 0 & 0 & 0 & 0 & 6 & 0 \end{pmatrix} \quad (2.3.3)$$

The actual number of particles of type k will be denoted by m_k . A quasi-particle has restricted values for momenta, depending on the number of particles $\mathbf{m} = (m_1, m_2, \dots, m_t)$ of each type. This is to be compared with ordinary particles which take on unrestricted values for their momenta. There is a Pauli exclusion principle which applies to these fermionic particles so that each state available can only be occupied by a single particle. The states that are not occupied by quasi-particles are referred to as *hole states*. There is in fact a duality between particles and holes. The hole states can be viewed as *dual quasi-particles*. There are t types of dual quasi-particles corresponding to the t types of quasi-particles. The actual number of dual quasi-particles of type k is denoted by n_k so the numbers of dual particles is given by $\mathbf{n} = (n_1, n_2, \dots, n_t)$.

It is now clear that for a quasi-particle of type k there are $m_k + n_k$ states available (m_k occupied states and n_k holes) so, allowing for t independent types, the total number of ways of occupying the fermionic states is

$$\binom{m_1 + n_1}{m_1} \binom{m_2 + n_2}{m_2} \dots \binom{m_t + n_t}{m_t} = \prod_{k=1}^t \binom{m_k + n_k}{m_k} \quad (2.3.4)$$

The relations between the numbers of quasi-particles \mathbf{m} and \mathbf{n} , which involve the system size N are called the (\mathbf{m}, \mathbf{n}) system.

2.3.2 Gaussian Polynomials

The Gaussian polynomials or q -binomials are defined by

$$\left[\begin{matrix} m+n \\ m \end{matrix} \right]_q = \left[\begin{matrix} m+n \\ n \end{matrix} \right]_q = \begin{cases} \frac{(q)_{m+n}}{(q)_m (q)_n} & m, n \text{ non-negative integers} \\ 0 & \text{otherwise} \end{cases} \quad (2.3.5)$$

so from (2.2.3),

$$\frac{(q)_{m+n}}{(q)_m (q)_n} = \frac{\prod_{j=n+1}^{m+n} (1 - q^j)}{\prod_{j=1}^m (1 - q^j)} \quad (2.3.6)$$

For example, some q -binomial coefficients are

$$\left[\begin{matrix} 2 \\ 1 \end{matrix} \right]_q = \frac{1 - q^2}{1 - q} = 1 + q \quad (2.3.7)$$

$$\left[\begin{matrix} 3 \\ 1 \end{matrix} \right]_q = \left[\begin{matrix} 3 \\ 2 \end{matrix} \right]_q = \frac{1 - q^3}{1 - q} = 1 + q + q^2 \quad (2.3.8)$$

$$\left[\begin{matrix} 4 \\ 2 \end{matrix} \right]_q = \frac{(1 - q^3)(1 - q^4)}{(1 - q)(1 - q^2)} = 1 + q + 2q^2 + q^3 + q^4 \quad (2.3.9)$$

The Gaussian polynomials satisfy the identities

$$\left[\begin{matrix} N \\ M \end{matrix} \right]_{\frac{1}{q}} = q^{-M(N-M)} \left[\begin{matrix} N \\ M \end{matrix} \right]_q, \quad \lim_{N \rightarrow \infty} \left[\begin{matrix} N \\ a \end{matrix} \right] = \frac{1}{(q)_\infty} \quad (2.3.10)$$

where a is a constant. In the limit as $q \rightarrow 1$, the Gaussian polynomials become the familiar binomial coefficients.

$$\lim_{q \rightarrow 1} \begin{bmatrix} N \\ M \end{bmatrix}_q = \binom{N}{M} \quad (2.3.11)$$

The Gaussian polynomials can be interpreted in terms of particles and holes, or the number of ways to occupy a given number of fermionic states. For example, $\begin{bmatrix} 4 \\ 2 \end{bmatrix}_q$ describes the number of ways to occupy four fermionic states with two particles, so that there are therefore two holes. This can be interpreted diagrammatically as shown below. All of the possible occupations of particles and holes are shown with the particles shown as solid dots and the holes as empty dots.

$$\begin{bmatrix} 4 \\ 2 \end{bmatrix}_q = \begin{array}{ccccccccc} & 1 & + & q & + & 2q^2 & + & q^3 & + & q^4 & & \\ & \begin{array}{c} \circ \\ | \\ \circ \\ | \\ \bullet \\ | \\ \bullet \end{array} & \longrightarrow & \begin{array}{c} \circ \\ | \\ \bullet \\ | \\ \circ \\ | \\ \bullet \end{array} & \longrightarrow & \begin{array}{c} \circ \\ | \\ \bullet \\ | \\ \bullet \\ | \\ \circ \end{array} & \longrightarrow & \begin{array}{c} \bullet \\ | \\ \circ \\ | \\ \bullet \\ | \\ \circ \end{array} & \longrightarrow & \begin{array}{c} \bullet \\ | \\ \bullet \\ | \\ \circ \\ | \\ \circ \end{array} & & \\ & & & & & \begin{array}{c} \bullet \\ | \\ \circ \\ | \\ \circ \\ | \\ \bullet \end{array} & & & & & & \end{array} \quad (2.3.12)$$

If we regard the diagram as representing states of a certain energy, then we regard the first one as lowest energy; the particles are in the lowest available positions. Each different combination can then be seen as an excitation of the particles. A particle moving into an adjacent hole can be considered as an excitation of one unit of energy. We see that the diagram represents successive excitations; the first figure is the lowest state and we take this as the reference state so it has energy zero. Each particle interchange adds energy one. The second figure then is the excited state created by one movement of a particle to an adjacent hole; this then has energy one. The third figure, actually two figures on top each other, are the two excitation states that can be reached from the second figure. The top one is obtained by the particle at position one moving to the adjacent empty site at position two. However, the particle at position three is also able to move higher, to the empty site at position four. So there are two degenerate energy states of energy two. There is only one possible particle move from both of these states and that produces figure four, which also has only one particle move available to it. If we take q to the power of each of these energies, we have the q -binomial $1 + q + 2q^2 + q^3 + q^4$ as before.

The standard Gaussian polynomials $\left[\begin{matrix} N \\ M \end{matrix} \right]_q$ above are valid for m, n non-negative integers. We define now two extensions of this definition involving negative N, M . For non-negative N, M these agree with the standard Gaussian polynomials. The specific values allowing negative integers N, M are

$$\left[\begin{matrix} N \\ N \end{matrix} \right]_q^{(0)} = 1, \quad \left[\begin{matrix} N \\ 0 \end{matrix} \right]_q^{(0)} = 0 \quad N < 0 \quad (2.3.13)$$

$$\left[\begin{matrix} N \\ N \end{matrix} \right]_q^{(1)} = 0, \quad \left[\begin{matrix} N \\ 0 \end{matrix} \right]_q^{(1)} = 1 \quad N < 0 \quad (2.3.14)$$

Only the $\left[\begin{matrix} -1 \\ 0 \end{matrix} \right]_q^{(1)}$ will actually be used here.

2.3.3 Finitised Fermionic Characters

The ‘fundamental fermionic form’ [20, 24] for the (r, s) finitised character is given by

$$\chi_{r,s}^{(N)}(q) = q^{\Delta_{r,s}^{(p,p')} - c/24} F_{r,s}(q) \quad (2.3.15)$$

$$F_{r,s}^{(N)}(q) = q^\alpha \sum_{(\mathbf{m}, \mathbf{n})} q^{\frac{1}{2} \mathbf{m}^T \mathbf{B} \mathbf{m} + \mathbf{A}^T \mathbf{m}} \prod_{i=1}^t \left[\begin{matrix} ((\mathbf{I} - \mathbf{B})\mathbf{m} + N\mathbf{u}_0 + \mathbf{u}_1)_i \\ m_i \end{matrix} \right]_q^{(1)} \quad (2.3.16)$$

where \mathbf{I} is the identity matrix, \mathbf{B} is a fixed $t \times t$ matrix which depends on (p, p') , \mathbf{u} and \mathbf{A} are t -dimensional vectors which depend on (r, s) in addition to (p, p') . The dependence on the system size N enters only through the explicit dependence in $\mathbf{u} = N\mathbf{u}_0 + \mathbf{u}_1$. The constant α is chosen so that $F_{r,s}^{(N)}$ starts as $F_{r,s}^{(N)} = 1 + O(q)$. Here the sum is restricted by the (\mathbf{m}, \mathbf{n}) system which expresses the fact that the q -binomials arise from the counting of fermionic states as in (2.3.4)

$$\mathbf{m} + \mathbf{n} = (\mathbf{I} - \mathbf{B})\mathbf{m} + N\mathbf{u}_0 + \mathbf{u}_1 \quad (2.3.17)$$

2.3.4 Finitised Bosonic Characters

The bosonic forms of the characters for the minimal models also admit finitised forms. Explicitly,

$$\chi_{r,s}^{(N)}(q) = q^{\Delta_{r,s}^{(p,p')} - c/24} B_{r,s}(q) \quad (2.3.18)$$

$$B_{r,s}^{(N)} = \sum_{n=-\infty}^{\infty} q^{n^2 pp' + n(p'r - ps)} \left[\begin{matrix} N \\ \frac{N+s-b}{2} - np' \end{matrix} \right] - q^{(np+r)(np'+s)} \left[\begin{matrix} N \\ \frac{N+s-b}{2} - np' - s \end{matrix} \right]$$

where

$$b = b(r) = \left\lfloor \frac{rp'}{p} \right\rfloor \quad (2.3.19)$$

We note that $B_{r,s}^{(N)}$ starts as $B_{r,s}^{(N)} = 1 + O(q)$.

2.3.5 Equivalence of Finitised Characters

When the undetermined quantities \mathbf{B} , \mathbf{A} , \mathbf{u}_0 and \mathbf{u}_1 are properly determined, the finitised fermionic characters agree precisely with the finitised bosonic characters and the one-dimensional configurational sums

$$F_{r,s}^{(N)}(q) = B_{r,s}^{(N)}(q) = X_N(s, b, b+1; q), \quad b = b(r) = \left\lfloor \frac{rp'}{p} \right\rfloor \quad (2.3.20)$$

Indeed, this relation can be used to find the quantities \mathbf{B} , \mathbf{A} , \mathbf{u}_0 and \mathbf{u}_1 .

The coincidence between the finitised fermionic characters and the one-dimensional configurational sums is remarkable because the parameter q in the finitised fermionic characters is the modular parameter of the critical ($\tilde{p} = 0$) model related to the geometry of an $M \times N$ strip

$$q = \exp \left[-\frac{M}{N} \pi \sin(p'u) \right] \quad (2.3.21)$$

whereas the parameter q in the one-dimensional configurational sums is related through $\tilde{p} \neq 0$ to the departure off-criticality. These two quantities q are *not* the same though they appear the same way in these formulas. The reason behind this coincidence will become clearer in Chapter 4 when we discuss the physical combinatorics.

Clearly, the finitised characters reproduce the full conformal characters in the limit $N \rightarrow \infty$

$$\chi_{r,s}(q) = \lim_{N \rightarrow \infty} \chi_{r,s}^{(N)}(q) \quad (2.3.22)$$

Chapter 3

Physical Combinatorics of Critical Forrester-Baxter Models

In Chapter 2, we constructed one-dimensional configurational sums combinatorially from the local energies of the critical Forrester-Baxter models, as polynomials of the form $\sum_E q^E$ that generate the energies of N -step paths on $p' - 1$ heights. In Chapter 3, we saw that one-dimensional configurational sums coincide with finitized bosonic and fermionic characters. The fermionic forms have the virtue that they encode information on the particle content of the theory. In this chapter, we will identify the finitized fermionic characters as the spectra generating functions associated with the double-row transfer matrices. This will naturally lead to a combinatorial interpretation of the allowed *physical* fermionic states and their associated (\mathbf{m}, \mathbf{n}) systems. This combinatorial interpretation of physical states is called *physical combinatorics*.

Fused transfer matrices and strips

Given an $\mathcal{M}(p, p')$ lattice model with commuting transfer matrices

$$\mathbf{D}(u) = \mathbf{D}^1(u) \tag{3.0.1}$$

it is possible to construct, using the process of fusion [21], a sequence of level- k mutually commuting transfer matrices

$$\mathbf{D}^k(u), \quad k = 1, 2, \dots, t; \quad [\mathbf{D}^j(v), \mathbf{D}^k(u)] = 0 \tag{3.0.2}$$

where t is the total number of quasi-particles given by (2.3.2). We need not be concerned here with the details of this construction, but essentially the level- k fused transfer matrices are formed by fusing together $1 \times k$ face weights. Since these fused models satisfy a generalized Yang-Baxter equation, so they are all exactly integrable. In solving for certain properties of the original model (fundamental fusion level) it is often convenient to study the whole fusion hierarchy simultaneously. This is what we will do here in studying the physical combinatorics.

Each of the fused transfer matrices $\mathbf{D}^k(u)$ has associated with it a vertical strip, called the *physical strip*, in a complex u -plane. There is one complex plane for each fusion level k . For convenience, we usually take all of these physical strips to be $-\lambda < \operatorname{Re} u < \lambda$.

Eigenvalues as Laurent polynomials

The entries of the fused transfer matrices $\mathbf{D}^k(u)$ are all Laurent polynomials in $z = e^{iu}$ and are period functions of u with real period π . Since these matrices all mutually commute, they have a common set of eigenvectors independent of u . For finite system sizes N , these eigenvectors can be obtained numerically. By acting with the transfer matrices on the given eigenvectors one can obtain the eigenvalues $\Lambda(u)$ as Laurent polynomials in z with numerical coefficients. Using Mathematica, it is then straightforward to find numerically the zeros of these polynomials. The pattern of these zeros in the complex u plane, then characterises the eigenvalue. In the continuum scaling limit these eigenvalues give the energies of the associated CFT

Let us now discuss in more detail the patterns of zeros in the complex u -plane. Typically, these zeros are structured into units called *strings*. A 1-string consists of a single zero (usually in the centre of the physical strip) and a 2-string consists of two zeros with the same imaginary part (often but not always at the edges of the physical strip). Such strings occur in the complex u -plane associated with the transfer matrices at each fusion level. For example, the pattern of zeros of the ground state often consists of many 2-strings at the edges of the physical strip of the fundamental transfer matrix $\mathbf{D}^1(u)$. We refer to the physical strip of the fused transfer matrix $\mathbf{D}^k(u)$ as simply the strip k . From the symmetries of the $\mathcal{M}(p, p')$ lattice models, the patterns of zeros are symmetric under reflection about the real axis. Consequently, the graphs displayed in this Chapter only show the patterns of zeros in the upper half u -plane.

Particle content

Clearly, each strip is associated with a kind of quasi-particle. The details of this correspondence varies from model to model and we will discuss some cases below in detail. Generically however, there are at least two types of strings in a given strip, say 1-strings and 2-strings. There are a number of positions (given by the imaginary part of u) and the 1- and 2-strings are distributed among these positions. Combinatorially, this situation is precisely described by the Gaussian polynomials (2.3.12). The actual number of particles (say 2-strings) and dual particles (holes or 1-strings), that is the *particle content*, is controlled by the (\mathbf{m}, \mathbf{n}) system. Here the number of particles (2-strings) in each strip is n_k and the number of dual particles (1-strings) in each strip is m_k . Under duality, the role of the 1- and 2-strings (particles and dual particles) is interchanged.

Relating the path diagrams and the zero plots.

In Chapter 2 we discussed the energies of the models by defining a set of rules assigning weights to features in the path diagram. We have also the patterns of zeros, that, treated as strings, interprets the energies in terms of particles. We therefore have two objects that are both related to the energy of the model $\mathcal{M}(p, p')$ and we would like to connect the objects themselves. With that end in mind, in the rest of this Chapter we will discuss in some detail the physical combinatorics for the cases $\mathcal{M}(2, 5)$, $\mathcal{M}(2, 7)$, and $\mathcal{M}(4, 7)$. We will also consider the relation between $\mathcal{M}(4, 7)$ and $\mathcal{M}(3, 7)$ under the duality.

3.1 $\mathcal{M}(2, 5)$

The continued fraction decomposition of $\mathcal{M}(2, 5)$ is

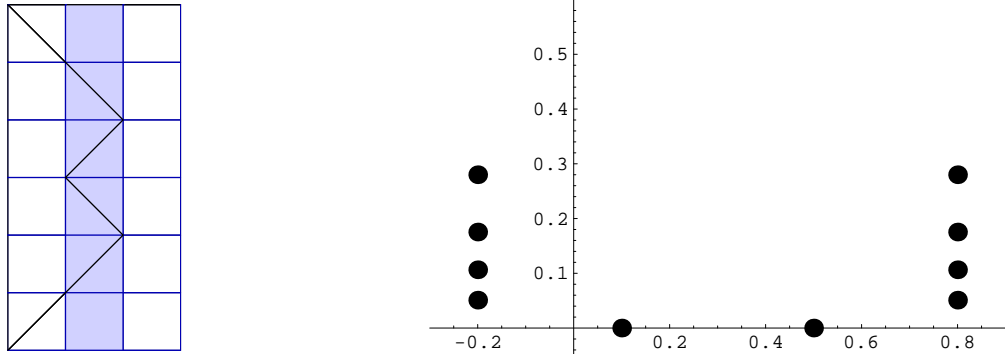
$$\frac{5}{2} = 1 + 1 + \frac{1}{0 + 1} \quad (3.1.1)$$

This has $\nu_0 = 1$, $\nu_1 = 0$, and $n = 1$ so $t = 1$ also. As t is the number of kinds of quasi-particles or strips, $\mathcal{M}(2, 5)$ has only one kind of particle. These particles and their dual particles occur in one physical strip; we call this a *one-strip model*. The patterns of the zeros are the simplest to understand when we only consider one strip.

We compare the path diagrams and the graphs of strings for $N = 6$. In the graphs, N is the system size and relates n_k and m_k ; here we have only m_1 and n_1 . We observe three kinds of strings present in the strip: “1-strings”, “short 2-strings”, and “long 2-strings”. $\mathcal{M}(2, 5)$ has only a single 1-string in the graphs, the single zero in the centre of the strip and furthest from the real axis. This 1-string is present at the same position in all of the graphs except the first one; it does not affect the excitation energies and we call it a “spectator”. The 2-string that sits on the real axis is also a spectator. In further discussion of these graphs for $\mathcal{M}(2, 5)$, ‘furthest from the real axis’ will be used to mean the string having the greatest imaginary part, excluding the 1-string spectator.

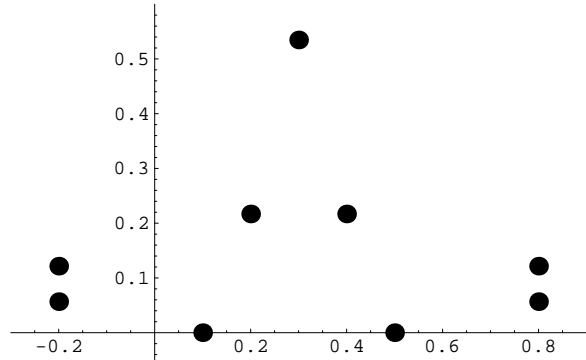
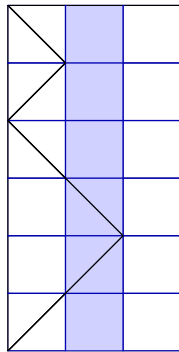
There are five paths for $N = 6$, with no degeneracies in the energies. The paths are in order of increasing energies as marked, and the graphs in the order of decreasing eigenvalues. The path diagrams are rotated to more easily compare them with the graphs. The terms ‘steps’ and ‘heights’ will be used as in Chapter 2. i.e. the top line is a or the zero-th step, and the steps increase downwards. Heights are now horizontal distances starting from 1 at the left edge of the path diagram. Paths in $\mathcal{M}(2, 5)$ are simply weighted: valleys in the lower outside region and peaks in the upper outside region have weight one. Note that in this orientation valleys now point left and peaks point right. For simplicity we will refer to ‘non-zero weighted features’ as ‘weighted features’ unless explicitly stated otherwise.

$$k = 1, \quad E = 0$$



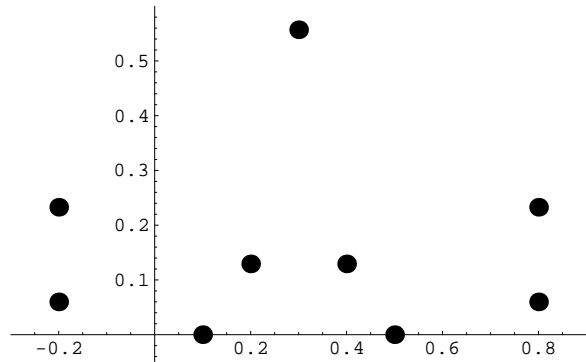
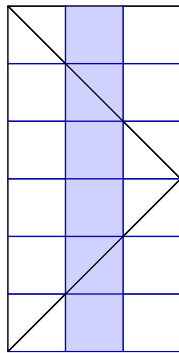
This is the lowest energy path for $N = 6$; we have already seen this path in 1.2.2. The path remains as much as possible within an odd band where there are no weighted features. In the graph, the two aligned rows of particles are rows of long 2-strings. There are no short 2-strings present.

$$k = 2, \quad E = 2$$



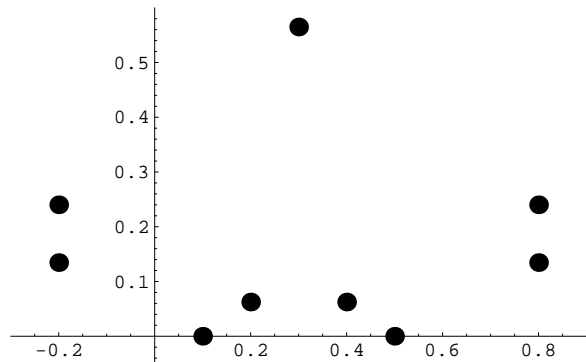
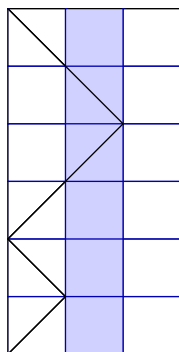
The path now has one weighted feature: the valley of weight 1, at step 2 (in the lower outside region). The path then enters the odd band and has no more weighted features. We observe that two of the long 2-strings have disappeared and we have instead one short 2-string, furthest from the real axis.

$$k = 3, \quad E = 3$$



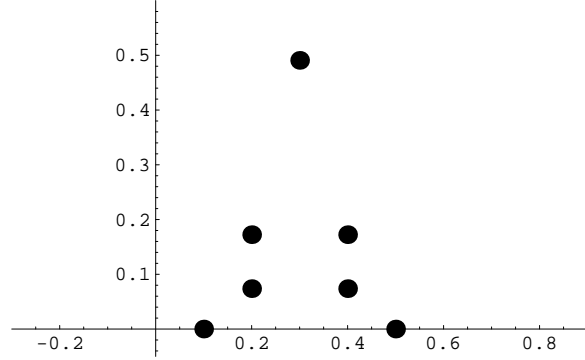
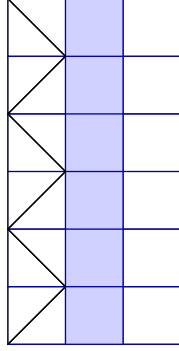
The path has again one weighted feature, now a peak of weight 1 at step 3. The short 2-string has interchanged one position with the long 2-string immediately below it.

$$k = 4, \quad E = 4$$



The path has one weighted feature, a valley of weight 1 at step 4, and the short 2-string has once again interchanged position with the long 2-string immediately below it. The short 2-string is now the closest of the strings to the real axis. (Excepting the real 2-string spectator.)

$$k = 5, \quad E = 6$$



There are now two weighted features in the path diagram: two valleys of weight 1 at steps 2 and 4. The graph has now no long 2-strings; two short 2-strings are the only strings present that contribute energy.

It seems clear that there is a connection between the features of the path and the strings of the diagram. The lowest energy state has no features with non-zero weights and no short 2-strings. The energy increases, and one feature of weight 1 and one short 2-string appears. These occur at the same relative heights; they start as the furthest elements of the path/graph from the endpoint/real axis and move progressively downwards with increases in energy. Then when there is no further opportunity to move downwards, a second feature of weight 1 and a second short 2-string appear together.

We therefore define the apparent relation between the path and the strings as follows: the weighted features in the path correspond to a short 2-string at the same relative position on the graph. (The weighted features are valleys in band 1 and peaks in band 3, each of weight one.) Crossing the odd centre band corresponds to a long 2-string.

Deducing a fermionic finitised character form

In chapter 2 we constructed the one dimensional configurational sums, and in Chapter 3 we stated that this sum is equivalent to a finitised conformal character of a minimal model. The general form of the fermionic finitised character is 2.3.16

$$F_{r,s}^{(N)}(q) = q^\alpha \sum_{(\mathbf{m}, \mathbf{n})} q^{\frac{1}{2} \mathbf{m}^T \mathbf{B} \mathbf{m} + \mathbf{A}^T \mathbf{m}} \prod_{i=1}^t \left[\begin{matrix} ((\mathbf{I} - \mathbf{B})\mathbf{m} + N\mathbf{u}_0 + \mathbf{u}_1)_i \\ m_i \end{matrix} \right]_q^{(1)} \quad (3.1.2)$$

The summation is over the (\mathbf{m}, \mathbf{n}) system, and the product of Gaussian polynomials has t components, each containing information about one of the t types of quasi-particles.

We see the same behaviour in the behaviour of the strings as in the combinatorial description of the Gaussian polynomials 2.3.12 as systems with occupied sites. Following this interpretation, in our graphs the short 2-strings appear to behave as the hole states and the long 2-strings as the occupied states. The significance of this is that the strings in our graphs also seem to contain information about the quasi-particles. Hence, although we don't have explicit values or relations for \mathbf{B}, \mathbf{A} or \mathbf{u} , we might have the information to nevertheless construct the finitised characters. We replace the \mathbf{u} -dependent relation in the Gaussian polynomials with an explicit expression for the (\mathbf{m}, \mathbf{n}) system:

$$\left[\begin{matrix} m_k + n_k \\ m_k \end{matrix} \right]_q^{(1)} \quad (3.1.3)$$

Using our comparison between the movements of strings and the combinatorics of the Gaussian polynomials, we can interpret the \mathbf{m} and $\mathbf{m} + \mathbf{n}$ from the graphs and use these in the general fermionic character. We then use the equivalency of the fermionic finitised characters and the one point configurational sums to determine the unknown \mathbf{B} and \mathbf{A} .

We firstly go through this process for $\mathcal{M}(2, 5)$, where there is only one term in the product of the Gaussian polynomials.

For $\mathcal{M}(2, 5)$ we interpret long 2-strings as occupied states or n_k and short 2-strings as hole states, or m_k . The first graph has four long 2-strings and no short 2-strings; there is only one arrangement of four filled states and it is represented by $\begin{bmatrix} 4 \\ 0 \end{bmatrix}_q^{(1)}$. The second graph has one short 2-string and two long 2-strings. There are three strings in total, so there are three different arrangements for this and we see the other two arrangements in the third and fourth graphs. These graphs together can be then be interpreted as $\begin{bmatrix} 3 \\ 1 \end{bmatrix}_q^{(1)}$. The fifth graph

has two short 2-strings; there is only one arrangement of two empty states, so we take $\begin{bmatrix} 2 \\ 2 \end{bmatrix}_q^{(1)}$. There are no more empty sites in the system; this last graph has the highest energy in our combinatorial interpretation, and it represents the state of highest energy for $N = 6$.

Placing these Gaussian polynomials into the general finitised fermionic character and substituting the corresponding m -value into the power of q , we obtain

$$F_{1,1}^{(6)}(q) = q^{\frac{1}{2}(0)\mathbf{B}(0)+\mathbf{A}^T(0)} \begin{bmatrix} 4 \\ 0 \end{bmatrix}_q^{(1)} + q^{\frac{1}{2}(1)\mathbf{B}(1)+\mathbf{A}^T(1)} \begin{bmatrix} 3 \\ 1 \end{bmatrix}_q^{(1)} + q^{\frac{1}{2}(2)\mathbf{B}(2)+\mathbf{A}^T(2)} \begin{bmatrix} 2 \\ 2 \end{bmatrix}_q^{(1)} \quad (3.1.4)$$

\mathbf{B} and \mathbf{A} are scalars for one strip models. We express them as $\mathbf{B} = b$ and $\mathbf{A} = a$ and equate this to $X_6(1, 1, 2; q) = 1 + q^2 + q^3 + q^4 + q^6$.

$$F_{1,1}^{(6)}(q) = 1 + q^{\frac{b}{2}+a}(1 + q + q^2) + q^{2b+2a} \quad (3.1.5)$$

$$= 1 + q^2 + q^3 + q^4 + q^6 \quad (3.1.6)$$

$$\Rightarrow \begin{cases} a + \frac{b}{2} & = 2 \\ 2b + 2a & = 6 \end{cases} \quad (3.1.7)$$

Therefore $b = \frac{1}{2}$ and $a = 1$. We still need to find the relation between \mathbf{n} and \mathbf{m} , as we wish to express the character more generally, and as a function of one of these variables only. From

$\begin{bmatrix} 4 \\ 0 \end{bmatrix}_q^{(1)}$ we obtain $m = 0$, $m + n = 4$; from $\begin{bmatrix} 3 \\ 1 \end{bmatrix}_q^{(1)}$ we obtain $m = 1$, $m + n = 3$; and from

$\begin{bmatrix} 2 \\ 2 \end{bmatrix}_q^{(1)}$ we have $m = 2$, $m + n = 3$. $N = 6$ for all of these and so we have $n + m = N - 2 - m$

or the (\mathbf{m}, \mathbf{n}) system:

$$m = \frac{1}{2}(N - 2 - n) \quad (3.1.8)$$

or

$$n = N - 2 - 2m \quad (3.1.9)$$

We therefore deduce the finitised character for $\mathcal{M}(2, 5)$ to be

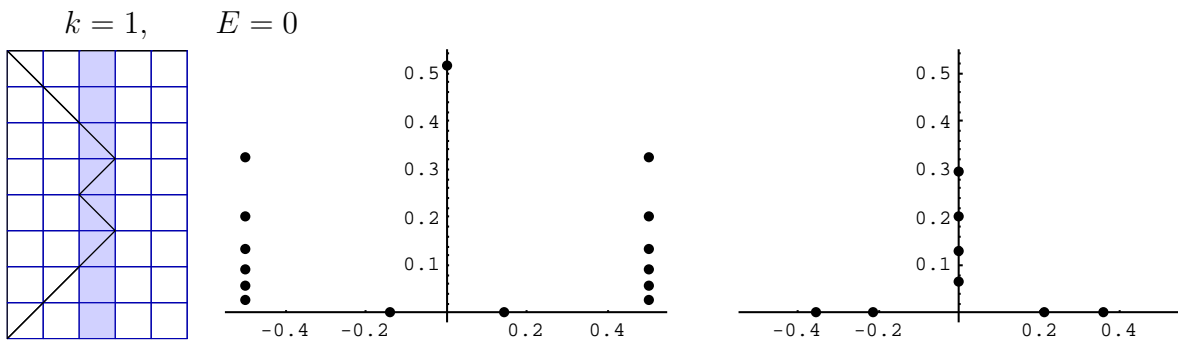
$$\chi^{(N)}(q) = \sum_m q^{m^2+m} \left[\begin{matrix} N-2-m \\ m \end{matrix} \right]_q^{(1)} \quad (3.1.10)$$

Comparing this against both the bosonic finitised character and the one-point configuration sums for system sizes up to 16, we find that they are equal. Thus we put forward the hypothesis that we have constructed the fermionic finitised character by physical combinatorics of the patterns of zeros. We need to look at more detailed examples to be more confident of this.

3.2 $\mathcal{M}(2, 7)$

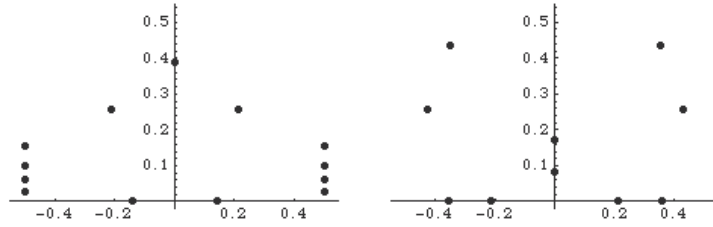
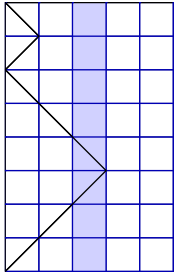
$\mathcal{M}(2, 7)$ has $\nu_0 = 2$, $\nu_1 = 0$, $n = 1$. This gives $t = 2$; it is a two strip model. We observe m_1 and n_1 in the first strip and m_2 and n_2 in the second strip. This added dimension will give us a more complex relation between the paths and the strings, testing our hypothesis. We need to look at a system of size of at least $N = 8$ to observe the behaviour in the second strip. There are 14 paths for $N = 8$. The weighting rules for the paths are very simple; they are the same as for $\mathcal{M}(2, 5)$.

We index the path diagrams because the i -th path diagram does not always relate to the i -th graph. The paths are always in increasing order of energy, but some of the graphs are not. This effect is because there is a forced disorder in the zeros of the eigenvalues from the restricted system size. As N increases to ∞ this disorder will vanish and the graphs (which are in order of decreasing eigenvalues) will be ordered exactly as the paths. Here they have been interchanged where necessary so that each path diagram is presented with the related graph.

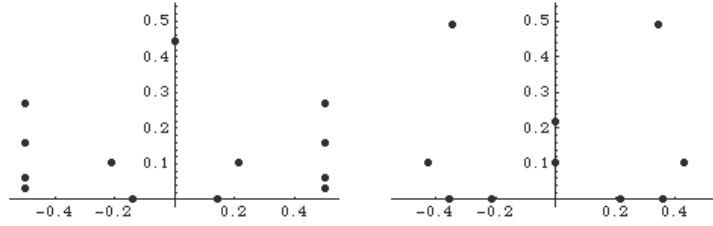
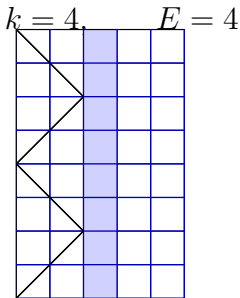
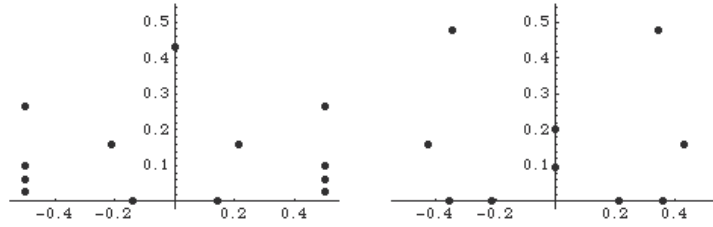
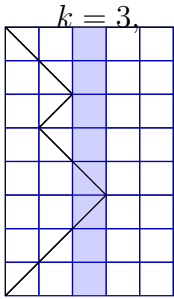


We observe a similar situation to that for the first path in $\mathcal{M}(2, 5)$. The path is in its lowest energy state and has weight zero. In the first strip there are the spectators as for $\mathcal{M}(2, 5)$; a 1-string furthest from the real axis and a 2-string on the real axis. These aside, we observe six long 2-strings. In the second strip there are four 1-strings and what appears to be two sets of 2-strings on the real axis. We expect these 2-strings to behave as spectators. We conjecture from the previous example that we will next observe a different kind of string appear in the first strip in the place of the highest two 2-strings.

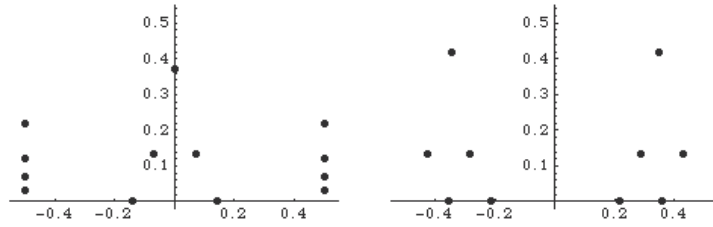
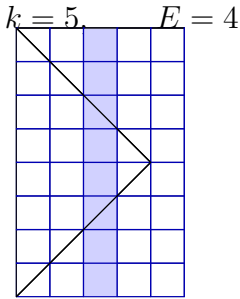
$k = 2, \quad E = 2$



The first strip has the expected short 2-string appear. The second strip now has only two 1-strings, and different strings appear in the second strip as well. There is one 2-string high on the complex axis, and another slightly wider 2-string lower down. The first 2-string appears in all of the rest of the graphs for $N = 8$ so we label it a spectator. The second 2-string is at the exact height of the short 2-string in the first strip. We believe there is some overlap between the strips, and that this string is a ‘ghost’ of the short 2-string in the same strip. In the next few graphs it can be seen that there is always a string like this in the second strip, at the same height as a short 2-string in the first. We will call such strings ‘ghost strings’. We imagine two vertical lines placed at ± 0.4 on the real axis. We will only consider strings *within* these lines as belonging to the second strip and contributing energies. The short 2-string is again at the same relative position as the valley of weight one in the path.

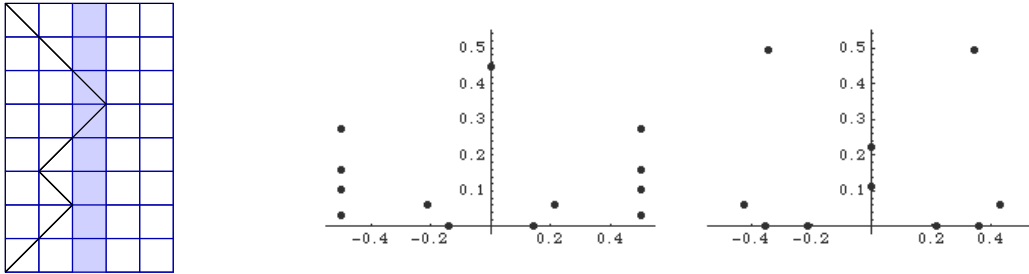


These two paths have a valley of weight one that shifts downwards, and the graphs have a short 2-string that similarly interchanges position to move downwards.



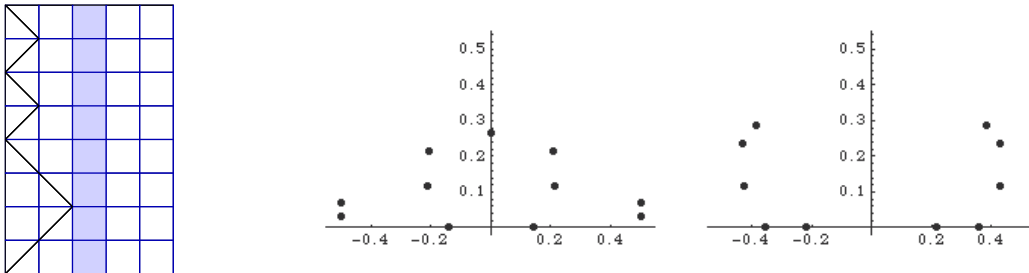
This case is unique (for $N = 8$) for both the path and the graph. It is the only path to cross the centre band and appear in the upper outside region. It is also the only graph to have a different type of string appear in the second strip; we now have a long 2-string. (We note that there are actually two 2-strings that appear and that the longer 2-string is a ghost string.) Naturally we relate these two appearances.

$$k = 6, \quad E = 5$$



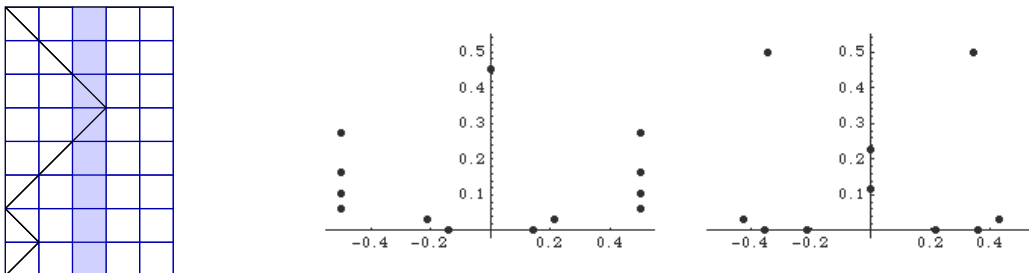
We see that the short 2-string is moving downwards via a series of interchanges that take the system to a higher energy state. The single non-zero weighted feature in the path shifts downwards in tandem. The paths for $k = 2, 3, 4, 6$ and 8 furnish the complete set of combinations that express $\begin{bmatrix} 5 \\ 1 \end{bmatrix}_q$.

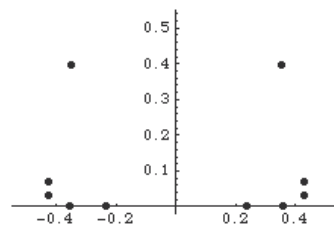
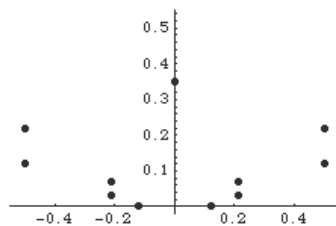
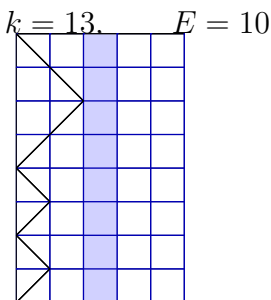
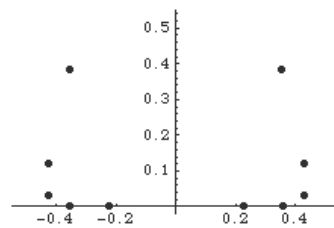
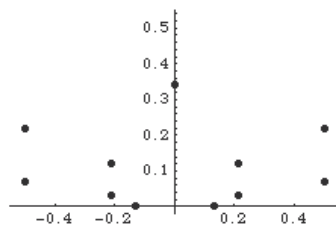
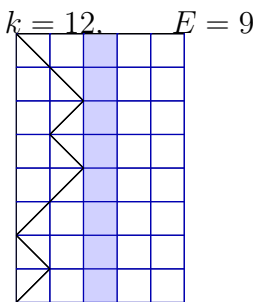
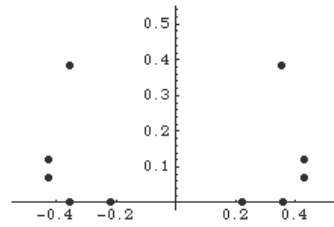
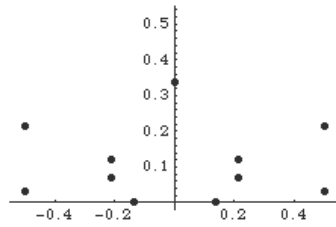
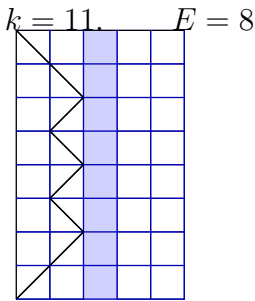
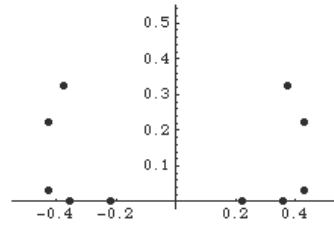
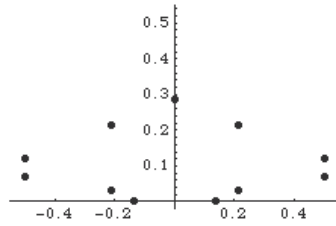
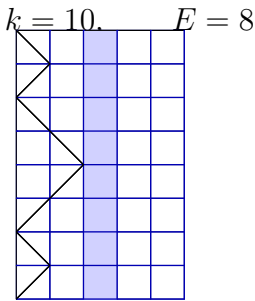
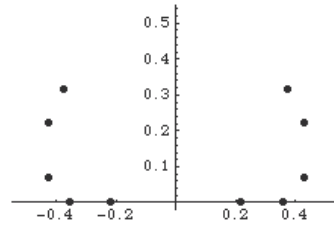
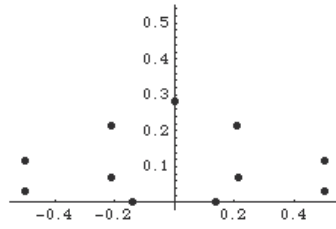
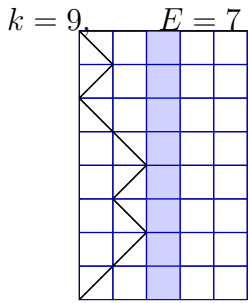
$$k = 7, \quad E = 6$$



This path and paths of $k = 9, 10, 11, 12, 13$ all have two valleys of weight 1 in the path and two short 2-strings in the graph, at the same heights relative to the rest of the path/graph. There are no strings in the second strip.

$$k = 8, \quad E = 6$$

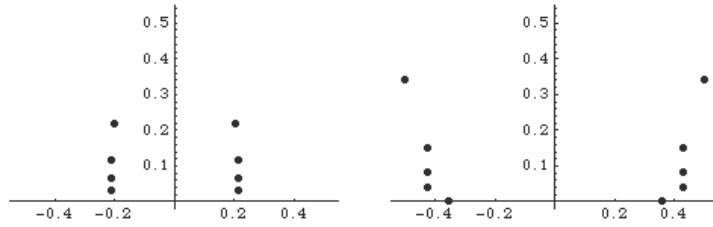
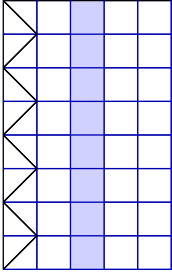




The combination of interchanges in the first strip of the five graphs immediately above and the graph for $k = 7$ is exactly that in the example of the Gaussian polynomials 2.3.12. We

therefore interpret these six diagrams as $\left[\begin{matrix} 4 \\ 2 \end{matrix} \right]_q$.

$k = 14, E = 12$



This graph has three non-zero weighted features on the path and three short 2-strings in the first strip on the graph.

The example of $\mathcal{M}(2, 7)$ supports our theory of a relation between the short 2-strings or hole states and the weighted features of the path. Until now we have only seen weighted features in the lower outside region. The single weighted feature in path 5 is a peak in the upper outside region, above the single odd centre band. This peak also coincides with the only appearance of an 2-string in the second strip. As the corresponding Gaussian polynomials drawn from strip 1 account exactly for all paths except this one, we deduce that the 1-strings in strip 2 are unexcited particles and do not contribute. We note that the 1-strings in the second strip always occur in pairs.

The relation we claim between the path and the strings in two strips is more subtle. Now that we have two kinds of particles (and their duals), we split the path diagram and make the assumption that generally, but not always, we consider the upper half in relation to strip 2 and the lower half in relation to strip 1. A key point that reinforces our interpretation of the strings as excitation states is that non-zero weighted features correspond to what we term excited particles, and zero weighted features correspond to unexcited particles.

Strip 1 contains much more information; in the lower half of the path we immediately relate the valleys of weight 1 with short 2-strings in strip 1. We map slants across the two even bands, and every crossing of the odd centre band to a long 2-string. Crossing the centre odd band is related with long 2-strings as for $\mathcal{M}(2, 5)$ and also slants across the even bands 1 and 2. We note that these are both zero-weighted features. The relation between the features and strip 2 is a little more subtle. The long 2-strings are the hole states and relate to peaks above the centre band. Peaks that are within the odd centre band map to pairs of 1-strings, except for the path $k = 4$. This path has no peak in the odd band and one pair of 2-strings in the second strip. We claim that this pair of 2-strings comes from the valley at step 4 accompanied by the two slants on either side. One way to think of this is as an upside-down peak, that if inverted would be a peak in the upper outside region. This object may seem artificial and it is the exception to our ‘splitting’ of the path into two strip; it is the only such object in the set of paths for $N = 8$ and using it gives us a precise relation between each path and a single graph. For reasons of time we do not give the case $N = 12$ here, but this new feature is needed again here to give precise path/graph relations.

The form of the Gaussian polynomial (for strip 2) is $\begin{bmatrix} m_2 + n_2 \\ m_2 \end{bmatrix}_q$; the 1-strings should correspond to one of these m or n , in order to give us Gaussian polynomials with a single combinatorial description: $\begin{bmatrix} m_2 + n_2 \\ m_2 \end{bmatrix}_q$ or $\begin{bmatrix} m_2 + n_2 \\ n_2 \end{bmatrix}_q$. Given that the paths are in (gener-

ally) order of increasing energy, we interpret the second kind of string that appears in strip 2 in the graph accompanying path 8 as a hole state: m_2 .

Deducing a fermionic finitised character form

As before we interpret the strings in terms of Gaussians, and then use these Gaussians to deduce the finitised fermionic character. We will go through the process again, but in less detail for the second time. As $\mathcal{M}(2, 7)$ has two strips \mathbf{B} is now a (2×2) matrix and \mathbf{A} a 2-dimensional vector; we express them as

$$\mathbf{B} = \begin{pmatrix} a & b \\ c & d \end{pmatrix} \quad (3.2.1)$$

$$\mathbf{A} = \begin{pmatrix} e \\ f \end{pmatrix} \quad (3.2.2)$$

The product in the fermionic character 2.3.16 now has two Gaussian polynomials in the product: $\left[\begin{smallmatrix} m_1 + n_1 \\ m_1 \end{smallmatrix} \right]_q^{(1)} \left[\begin{smallmatrix} m_2 + n_2 \\ m_2 \end{smallmatrix} \right]_q^{(1)}$. From the combinatorics of the strings we obtain these Gaussian polynomials and use them in the character as for $\mathcal{M}(2, 5)$. The Gaussian polynomials we find from $N = 8$ are

$$\left[\begin{smallmatrix} 6 \\ 0 \end{smallmatrix} \right]_q^{(1)} \left[\begin{smallmatrix} 4 \\ 0 \end{smallmatrix} \right]_q^{(1)}, \quad \left[\begin{smallmatrix} 5 \\ 1 \end{smallmatrix} \right]_q^{(1)} \left[\begin{smallmatrix} 2 \\ 0 \end{smallmatrix} \right]_q^{(1)}, \quad (3.2.3)$$

$$\left[\begin{smallmatrix} 4 \\ 2 \end{smallmatrix} \right]_q^{(1)} \left[\begin{smallmatrix} 0 \\ 0 \end{smallmatrix} \right]_q^{(1)}, \quad \left[\begin{smallmatrix} 4 \\ 0 \end{smallmatrix} \right]_q^{(1)} \left[\begin{smallmatrix} 1 \\ 1 \end{smallmatrix} \right]_q^{(1)} \quad (3.2.4)$$

$$\left[\begin{smallmatrix} 3 \\ 3 \end{smallmatrix} \right]_q^{(1)} \left[\begin{smallmatrix} 0 \\ 0 \end{smallmatrix} \right]_q^{(1)} \quad (3.2.5)$$

We have to work through $N = 6$, $N = 8$ and $N = 10$ to find \mathbf{B} and \mathbf{A} . Equating our general form to the one dimensional configurational sum for $N = 6$ gives us $a = 1$, $e = 1$. From $N = 8$ we find $f = 4 - d$ and $N = 10$ further provides $c = 2 - b$. We put these into the fermionic character and sum over \mathbf{m} for $N > 10$ to obtain the details of these matrices. In order to do this we need the (\mathbf{m}, \mathbf{n}) system, which we determine from the Gaussian polynomials also: $n_1 + m_1 = N - 2 - m_1 - 2m_2$ and $n_2 + m_2 = N - 4 - 2m_1 - 3m_2$, or

$$n_1 = N - 2 - 2m_1 - 2m_2 \quad n_2 = N - 4 - 2m_1 - 4m_2 \quad (3.2.6)$$

$$m_1 = \frac{N}{2} - n_1 + \frac{1}{2}n_2 \quad m_2 = -\frac{1}{2}(2 - n_1 + n_2) \quad (3.2.7)$$

We find $a, b, c, e = 1$, and $d, f = 2$. This gives us a finitised fermionic character

$$\chi^{(N)}(q) = \sum_{\mathbf{m}} q^{\mathbf{mDm} + m_1 + 2m_2^2} \left[\begin{smallmatrix} N - 2 - m_1 - 2m_2 \\ m_1 \end{smallmatrix} \right]_q^{(1)} \left[\begin{smallmatrix} N - 4 - 2m_1 - 3m_2 \\ m_2 \end{smallmatrix} \right]_q^{(1)} \quad (3.2.8)$$

where

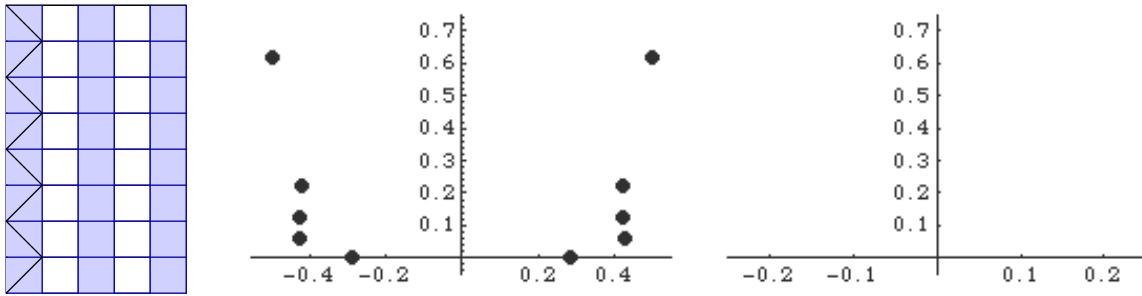
$$D = \begin{pmatrix} 1 & 1 \\ 1 & 2 \end{pmatrix} \tag{3.2.9}$$

When we compare this with the bosonic form and the one dimensional configurational sum we find that this is equivalent, for $N \leq 16$.

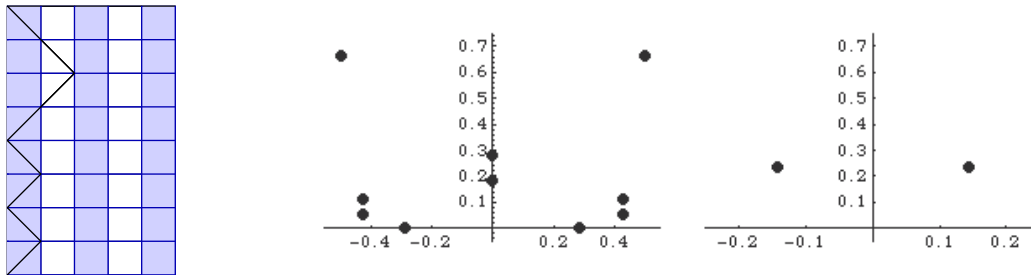
3.3 $\mathcal{M}(4, 7)$

The final example for which we compare the path diagrams and the patterns of zeros, and calculate the character combinatorially is $\mathcal{M}(4, 7)$. This is a 2-strip model, and has weighted features of peaks, valleys and slants only in the even bands.

$$k = 1, \quad E = 0$$

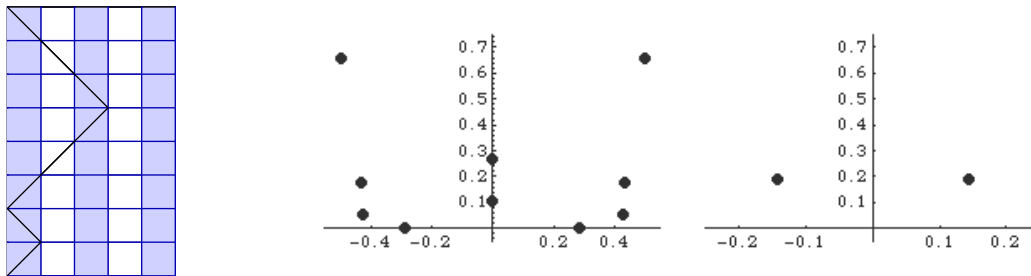


$$k = 2, \quad E = 2$$



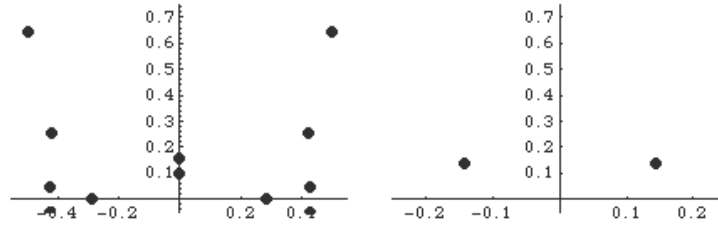
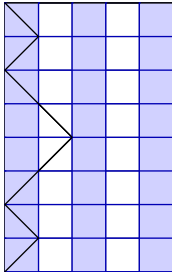
The appearance of a peak in an even band coincides with two new string kinds in the graph: a pair of one strings in the first strip and a two string in the second. As every kind of feature in the even band is weighted, we suggest that crossing the even band is related to a 1-string in the first strip, and the peak related to the appearance in the second.

$$k = 3, \quad E = 3$$

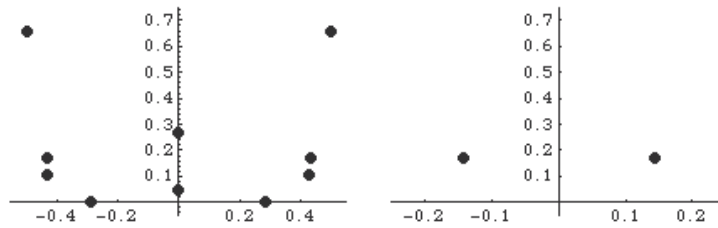
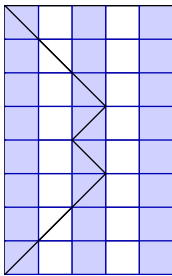


We see the same behaviour as above, with the difference that the peak that relates to the string in the second strip is now in an even band. This suggests that the relevant placement is between an odd and an even band.

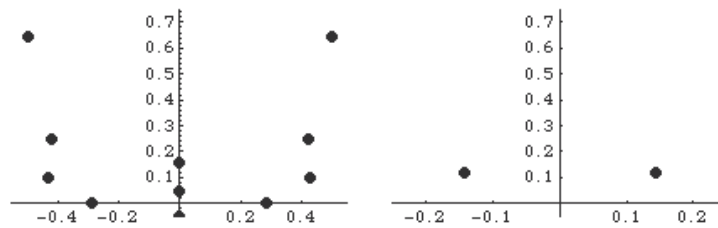
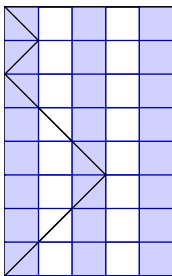
$$k = 4, \quad E = 4$$



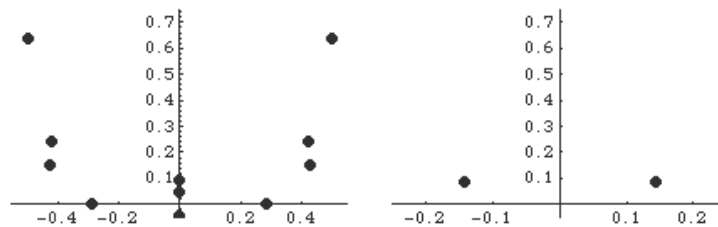
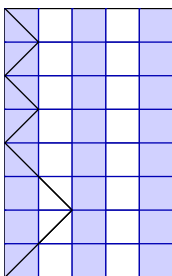
$$k = 5, \quad E = 4$$



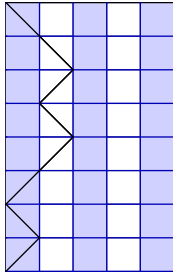
$$k = 6, \quad E = 5$$



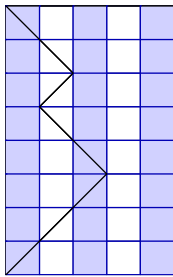
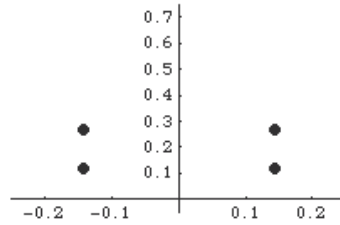
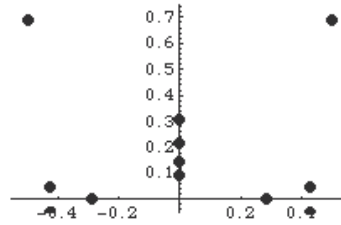
$$k = 7, \quad E = 6$$



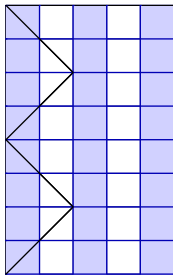
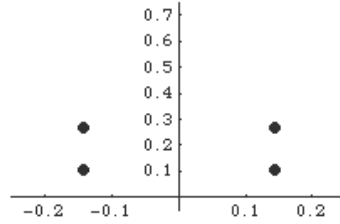
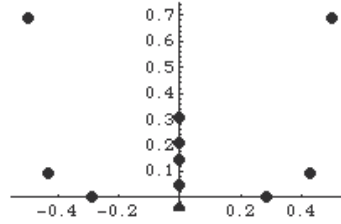
$$k = 8, \quad E = 6$$



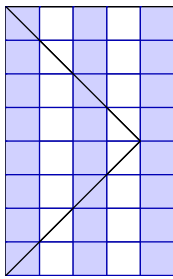
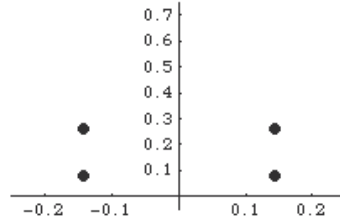
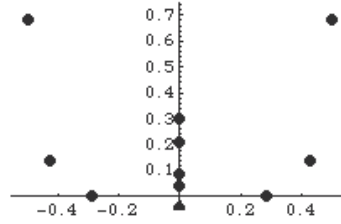
$k = 9, \quad E = 7$



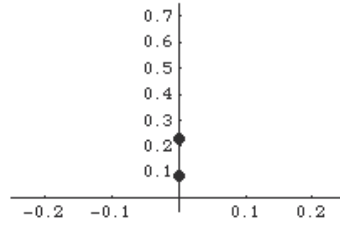
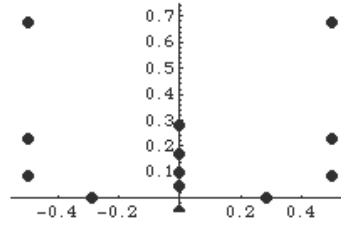
$k = 10, \quad E = 8$



$k = 11, \quad E = 8$



$k = 12, \quad E = 9$



We now see 1-strings appearing in strip 2. It is consistent with the previous examples considered that these are related to the features of the path in the upper half of the path diagram. This is the first path for $N = 8$ where we have such features; the peak at step 4 crosses into the 4th band and we relate this to the pair of 1-strings in strip 2. Moving across the centre odd band into the 4th band also corresponds to 2-strings in the first strip.

The Gaussian polynomials that we now interpret these strings as are

$$\begin{aligned} \begin{bmatrix} 3 \\ 0 \end{bmatrix}_q^{(1)} \begin{bmatrix} 0 \\ 0 \end{bmatrix}_q^{(1)}, & \quad \begin{bmatrix} 4 \\ 2 \end{bmatrix}_q^{(1)} \begin{bmatrix} 1 \\ 0 \end{bmatrix}_q^{(1)} \\ \begin{bmatrix} 5 \\ 1 \end{bmatrix}_q^{(1)} \begin{bmatrix} 2 \\ 0 \end{bmatrix}_q^{(1)} & \quad \begin{bmatrix} 6 \\ 4 \end{bmatrix}_q^{(1)} \begin{bmatrix} 2 \\ 2 \end{bmatrix}_q^{(1)} \end{aligned} \quad (3.3.1)$$

$$\begin{bmatrix} 6 \\ 6 \end{bmatrix}_q^{(1)} \begin{bmatrix} 3 \\ 0 \end{bmatrix}_q^{(1)} \quad (3.3.2)$$

Determining the finitised character from the combinatorics

Here we use n_1 and n_2 as the independent variables because the model $\mathcal{M}(4, 7)$ has $p < p' < 2p$. Once again we need to use the Gaussian polynomials deduced from the combinatorics for $N = 6$ and $N = 10$ in addition to those for the $N = 8$ case displayed above:

\mathbf{A} and \mathbf{B} are again put first in general terms :

$$\frac{1}{4}(n_1, n_2) \begin{pmatrix} a & b \\ c & d \end{pmatrix} \begin{pmatrix} n_1 \\ n_2 \end{pmatrix} + (e, f) \begin{pmatrix} n_1 \\ n_2 \end{pmatrix} \quad (3.3.3)$$

Starting with general functions to the finitised character for $N = 6$ gives $a = \frac{1}{4}$, $e = \frac{1}{2}$. Taking the Gaussian polynomials from the graphs for $N = 8$ and $N = 10$ still leaves a small number of equations with a large number of unknowns. A little experimentation gives \mathbf{A} and \mathbf{B} as

$$\frac{1}{4} \begin{pmatrix} a & b \\ c & d \end{pmatrix} = \frac{1}{4} \begin{pmatrix} 1 & 1 \\ -1 & 2 \end{pmatrix} \quad (3.3.4)$$

$$(3.3.5)$$

The \mathbf{B} found here for $\mathcal{M}(4, 7)$ is not unique; other matrices that give the same result are

$$\begin{pmatrix} 1 & -1 \\ 1 & 2 \end{pmatrix} \& \begin{pmatrix} 1 & 0 \\ 0 & 2 \end{pmatrix}$$

but we have chosen a matrix that is the same as that for the system of \mathbf{m} in terms of \mathbf{n} . So the (\mathbf{n}, \mathbf{m}) system for $\mathcal{M}(4, 7)$ is found from $n_1 + m_1 = \frac{1}{2}(N + n_1 - n_2) - 1$ and $n_2 + m_2 = \frac{n_1}{2}$ given by the Gaussian polynomials:

$$m_1 = \frac{N - n_1 - n_2}{2} - 1 \quad (3.3.6)$$

$$m_2 = \frac{1}{2}n_1 - n_2 \quad (3.3.7)$$

or

$$n_1 = \frac{2}{3}(N - 2m_1 + m_2 - 2)$$

$$n_2 = -\frac{1}{3}(-N + 2 + 2m_1 + 2m_2)$$

and n_1 and n_2 both have even parity. (This is observed in the graphs, and also it is the condition placed upon them when we check the character we find against the one dimensional configurational sums, so it holds for larger sizes than observed here.)

The \mathbf{B} found here for $\mathcal{M}(4, 7)$ is not unique; other matrices that give the same result are

$$\begin{pmatrix} 1 & 1 \\ -1 & 2 \end{pmatrix} \& \begin{pmatrix} 1 & 0 \\ 0 & 2 \end{pmatrix}$$

Here we choose a \mathbf{B} that is the same as that for the system of \mathbf{m} in terms of \mathbf{n} . So we find the character :

$$\chi^{(N)}(q) = \sum_{n_1, n_2, \text{both even}} q^{\frac{1}{4}(\mathbf{n}^T \begin{pmatrix} 1 & 1 \\ -1 & 2 \end{pmatrix} \mathbf{n} + 2n_1)} \left[\begin{matrix} \frac{N+n_1-n_2}{2} - 1 \\ n_1 \end{matrix} \right]_q \left[\begin{matrix} \frac{1}{2}n_1 \\ n_2 \end{matrix} \right]_q \quad (3.3.8)$$

The distinction of actual behaviour between \mathbf{m} or \mathbf{n} is not clear here; we could equally express the character in terms of the other. Here we have the character in terms of \mathbf{m} :

$$\chi^{(N)}(q) = \sum_{m_1 \text{ even}, m_2} q^{\frac{1}{8}\mathbf{m} \begin{pmatrix} 3 & -2 \\ -2 & 4 \end{pmatrix} \mathbf{m} + \frac{1}{2}m_1} \left[\begin{matrix} \frac{1}{2}(N - 2 + \frac{m_1}{2} + m_2) \\ m_1 \end{matrix} \right]_q^{(1)} \left[\begin{matrix} \frac{1}{2}m_1 \\ m_2 \end{matrix} \right]_q^{(1)} \quad (3.3.9)$$

and compared against the bosonic finitised character and the one dimensional configurational paths for up to $N = 16$ (which has 1341 paths), these give the same result.

3.4 Duality

$\mathcal{M}(4, 7)$ is the dual to $\mathcal{M}(3, 7)$. If we apply the dual transform $q \rightarrow \frac{1}{q}$, we should obtain the one from the other. This dual relation is an involution so either model can be mapped to the other by this transform. We use this to obtain $\mathcal{M}(3, 7)$ without going through all of the combinatorics. Generally if m is the independent variable used in one model, n is the independent variable in the dual, by convention. To do this we use the inverse of the matrix \mathbf{B} in the quadratic.

$$\begin{pmatrix} 3 & -2 \\ -2 & 4 \end{pmatrix}^{-1} = \frac{1}{2} \begin{pmatrix} 4 & 2 \\ 2 & 3 \end{pmatrix} \quad (3.4.1)$$

In the transformation $q \rightarrow \frac{1}{q}$ then,

$$\chi^{(N)}(q) = \sum_{m_1 \text{ even}, m_2} q^{-\frac{1}{8}\mathbf{m} \begin{pmatrix} 3 & -2 \\ -2 & 4 \end{pmatrix} \mathbf{m} - \frac{1}{2}m_1} \left[\begin{matrix} \frac{1}{2}(N - 2 + \frac{m_1}{2} + m_2) \\ m_1 \end{matrix} \right]_{\frac{1}{q}}^{(1)} \left[\begin{matrix} \frac{1}{2}m_1 \\ m_2 \end{matrix} \right]_{\frac{1}{q}}^{(1)} \quad (3.4.2)$$

expanded

$$\chi^{(N)}(q) = \sum_{m_1 \text{ even}, m_2} q^{-\frac{3}{8}m_1^2 + \frac{1}{2}m_1 m_2 - \frac{1}{2}m_2^2 - \frac{1}{2}m_1} \left[\begin{matrix} \frac{1}{2}(N - 2 + \frac{m_1}{2} + m_2) \\ m_1 \end{matrix} \right]_q^{(1)} \left[\begin{matrix} \frac{1}{2}m_1 \\ m_2 \end{matrix} \right]_q^{(1)} \quad (3.4.3)$$

becomes

$$\chi^{(N)}(q) = \sum_{m_1, m_2 \text{ even}} q^{-n_1^2 - n_1 n_2 - \frac{3}{4}n_2^2 - n_1 - \frac{1}{2}n_2} \left[\begin{matrix} \frac{1}{2}(N - 2 + \frac{m_1}{2} + m_2) \\ m_1 \end{matrix} \right]_{\frac{1}{q}}^{(1)} \left[\begin{matrix} \frac{1}{2}m_1 \\ m_2 \end{matrix} \right]_{\frac{1}{q}}^{(1)} \quad (3.4.4)$$

and recall the identity for $\left[\begin{matrix} m+n \\ n \end{matrix} \right]_{\frac{1}{q}}^{(1)}$:

$$\left[\begin{matrix} N \\ M \end{matrix} \right]_{\frac{1}{q}} = q^{-M(N-M)} \left[\begin{matrix} N \\ M \end{matrix} \right]_q \quad (3.4.5)$$

Then we have

$$\chi^{(N)}(q) = \sum_{m_1, m_2 \text{ even}} q^{-n_1^2 - n_1 n_2 - \frac{3}{4} n_2^2 - n_1 - \frac{1}{2} n_2 - m_1 n_1 - m_2 n_2} \left[\begin{matrix} \frac{1}{2}(N-2 + \frac{m_1}{2} + m_2) \\ m_1 \end{matrix} \right]_q^{(1)} \left[\begin{matrix} \frac{1}{2} m_1 \\ m_2 \end{matrix} \right]_q^{(1)} \quad (3.4.6)$$

and when the character is in terms of \mathbf{n} only, it is

$$\chi^{(N)}(q) = \sum_{m_1, m_2} q^{-n_1^2 - n_1 n_2 - \frac{3}{4} n_2^2 - n_1 - \frac{1}{2} n_2 - m_1 n_1 - m_2 n_2} \left[\begin{matrix} \frac{1}{2}(N-2 + \frac{m_1}{2} + m_2) \\ m_1 \end{matrix} \right]_{\frac{1}{q}}^{(1)} \left[\begin{matrix} \frac{1}{2} m_1 \\ m_2 \end{matrix} \right]_{\frac{1}{q}}^{(1)} \quad (3.4.7)$$

$$\chi^{(N)}(q) = \sum_{n_1, n_2 \text{ even}} q^{\frac{1}{4} \mathbf{n} \begin{pmatrix} 4 & 2 \\ 2 & 3 \end{pmatrix} \mathbf{n} + n_1 + \frac{1}{2} n_2} \left[\begin{matrix} N-2 - n_1 - n_2 \\ n_1 \end{matrix} \right]_q^{(1)} \left[\begin{matrix} \frac{1}{2} n_1 \\ n_2 \end{matrix} \right]_q^{(1)} \quad (3.4.8)$$

And we find this is equal to the fermionic finitised character for $\mathcal{M}(3, 7)$. We don't have combinatorics here to give us the parity restriction ' m_1, m_2 even' but we can see that this is a requirement from the Gaussian polynomials and the power of q .

3.5 Summary of Results

We present the finitised characters found for $\mathcal{M}(2, 5)$, $\mathcal{M}(2, 7)$, $\mathcal{M}(3, 7)$ and $\mathcal{M}(4, 7)$

$\mathcal{M}(2, 5)$

$$\chi^{(N)}(q) = \sum_m q^{m^2 + m} \left[\begin{matrix} N-2 - m \\ m \end{matrix} \right]_q^{(1)} \quad (3.5.1)$$

$\mathcal{M}(2, 7)$

$$\chi^{(N)}(q) = \sum_{\mathbf{m}} q^{\mathbf{m} \begin{pmatrix} 1 & 1 \\ 1 & 2 \end{pmatrix} \mathbf{m} + m_1 + 2m_2^2} \left[\begin{matrix} N-2 - m_1 - 2m_2 \\ m_1 \end{matrix} \right]_q^{(1)} \left[\begin{matrix} N-4 - 2m_1 - 3m_2 \\ m_2 \end{matrix} \right]_q^{(1)} \quad (3.5.2)$$

$\mathcal{M}(3, 7)$

$$\chi^{(N)}(q) = \sum_{n_1, n_2 \text{ even}} q^{\frac{1}{4} \mathbf{n} \begin{pmatrix} 4 & 2 \\ 2 & 3 \end{pmatrix} \mathbf{n} + n_1 + \frac{1}{2} n_2} \left[\begin{matrix} N-2 - n_1 - n_2 \\ n_1 \end{matrix} \right]_q^{(1)} \left[\begin{matrix} \frac{1}{2} n_1 \\ n_2 \end{matrix} \right]_q^{(1)} \quad (3.5.3)$$

$\mathcal{M}(4, 7)$

$$\chi^{(N)}(q) = \sum_{m_1, m_2 \text{ EVEN}} q^{\frac{1}{8} \mathbf{m} \begin{pmatrix} 3 & -2 \\ -2 & 4 \end{pmatrix} \mathbf{m} + \frac{1}{2} m_1} \left[\begin{matrix} \frac{1}{2} (N - 2 + \frac{m_1}{2} + m_2) \\ m_1 \end{matrix} \right]_q^{(1)} \left[\begin{matrix} \frac{1}{2} m_1 \\ m_2 \end{matrix} \right]_q^{(1)} \quad (3.5.4)$$

Conclusion

In this thesis we have studied combinatorial objects related to finitisations of the conformal characters of minimal models in CFT. This was carried out by looking at several examples.

We started with the Forrester-Baxter lattice models and discussed the construction of one dimensional configurational sums for the energies of the states in the model. We did this by assigning weights to features in the path of local heights, dependent on a banding structure to find the energy of each path. Remarkably, these one dimensional configurational sums precisely coincide with the finitised fermionic characters of minimal models in CFT.

Secondly, we compared the path diagrams of the local heights to the patterns of zeros of the eigenvalues of the transfer matrices for some of the $\mathcal{M}(2, 5)$, $\mathcal{M}(2, 7)$ and $\mathcal{M}(4, 7)$ Forrester-Baxter lattice models. We interpret units in these patterns as strings, and we observe a relation between these strings and features in the paths for the same models. The strings can be interpreted as particles whose numbers are controlled by the (\mathbf{m}, \mathbf{n}) system. This system is present in the finitised fermionic character in its fundamental form. From the strings we then have enough information to form unambiguously the finitised characters by comparison of the finitised fermionic forms to the one dimensional configurational sums.

We have thus described the finitised characters of the example minimal models in terms of the *physical combinatorics* of the patterns of zeros of the eigenvalues of the transfer matrices of the related lattice models. It would be very interesting to extend this study to the full set of minimal models. More insight into the (\mathbf{m}, \mathbf{n}) system would give us more information about the particle content of the models. It would also be beneficial if a general bijection between the paths and patterns of strings could be found, which would give us more insight into the relation between these objects.

Bibliography

- [1] I. Schur, S.-B Preuss. Akad. Wiss. Phys.-Math. Kl (1917) 302.
- [2] L.J. Rogers and S. Ramanujan, Proc. Camb. Phil. Soc. 19 (1919) 214.
- [3] E. Ising, Z. Phys. **31** (1925) 253
- [4] M.Takahashi and M.Suzuki, Prog. of Theo. Phys **48** (1972) 2187
- [5] R. J. Baxter, “Exactly Solved Models in Statistical Mechanics”. Academic Press, London, (1982)
- [6] A. A. Belavin, A. M. Polyakov and A. B. Zamolodchikov, Infinite conformal symmetry in two-dimensional quantum field theory. Nucl. Phys. **B241** (1984) 333
- [7] A.A.Belavin, A.M.Polyakov and A.B.Zamolodchikov, Infinite Conformal symmetry of critical fluctuations in two dimensions. J.Statist. Phys **34** (1984) 763
- [8] Friedan, Daniel; Qiu, Zongan; Shenker, Stephen Conformal invariance, unitarity, and critical exponents in two dimensions. Phys. Rev. Lett. 52 (1984), no. 18, 1575–1578
- [9] G. E. Andrews, R. J. Baxter and P. J. Forrester, Eight-Vertex SOS Model and Generalised Rogers-Ramanujan-Type Identities. J. Stat. Phys. **35** (1983) 193.
- [10] P. J. Forrester and R. J. Baxter, Further Exact Solutions of the Eight-Vertex SOS Model and Generalizations of the Rogers-Ramanujan Identities. J. Stat. Phys **38**(1985) 435-472.
- [11] A. Rocha-Caridi, in *Vertex Operators in Mathematics and Physics*, ed. J.Lepowsky, S.Mandelstam and I.M.Singer (Springer Berlin 1985)
- [12] H. Riggs, Solvable Lattice Models with Minimal and Nonunitary Critical Behaviour in Two Dimensions. Nucl. Phys. **B326** (1989) 673–688.
- [13] P.A.Pearce, Temperley-Lieb Operators and Critical *A-D-E* Models, Int. J. Mod. Phys. **4** (1990) 715.
- [14] F. Ravanini, R.Tateo and A.Valleriani, Dynkin TBAs. Int.J.Mod.Phys. A8 (1993) 1707-1728 1992

- [15] R.Kedem, T.R.Klassen, B.M.McCoy, and E. Melzer, Fermionic Sum Representations for Conformal Field Theory Characters, Phys.Lett. B372 (1996) 231-2351993
- [16] S. Dasmahapatra; R. Kedem; B. McCoy; E. Melzer, Virasoro characters from Bethe equations for the critical ferromagnetic three-state Potts model. (English summary) J. Statist. Phys. 74 (1994), no. 1-2, 239–274.
- [17] A. Berkovich and B.M.McCoy, Continued Fractions and Fermionic Representations for Characters of $\mathcal{M}(p, p')$ Minimal Models, hep-th/9412030 v4 1994 Lett.Math.Phys. 37 (1996) 49-66.
- [18] E. Melzer, Int. J. Mod. Phys. **A9** (1994) 1115 Fermionic character sums and the corner transfer matrix. (English summary) Internat. J. Modern Phys. A 9 (1994), no. 7, 1115–1136.
- [19] P. Di Francesco, P Mathieu and D. Sénéchal. Conformal Field Theory. Springer-Verlag, New York, 1997.
- [20] A. Berkovich, B.M.McCoy and A.Schilling, Rogers-Schur-Ramanujan Type Identities for the $\mathcal{M}(p, p')$ minimal models of Conformal Field Theory. J. Stat. Phys. **38** (1997) 435–472.
- [21] R.E. Behrend, P.A. Pearce and D.L. O’Brien, Interaction-Round-a-Face Models with Fixed Boundary Conditions: The ABF Fusion Hierarchy, J. Stat. Phys. **84** (1996)1–48.
- [22] O.Foda and T.Welsh, Melzer’s identities revisited, math.QA/9811156 1998
- [23] R.E. Behrend and P.A. Pearce, Integrable and Conformal Boundary Conditions for $sl(2)$ A - D - E Lattice Models and Unitary Minimal Conformal Field Theories, hep-th/0006094 (2000).
- [24] O. Foda and T.A.Welsh, On the combinatorics of Forrester-Baxter models, math.QA/0002100 (2000)
- [25] R.J.Baxter, The six and eight-vertex models revisited, cond-mat/0403138v1 2004